NASA CR-134840
R75AEG278

QUIET CLEAN SHORT-HAUL EXPERIMENTAL ENGINE (QCSEE) UNDER-THE-WING ENGINE COMPOSITE FAN BLADE DESIGN

May 1975

by

Advanced Engineering & Technology Programs Department
General Electric Company

(NASA-CR-134840) QUIET CLEAN SHORT-HAUL EXPERIMENTAL ENGINE (QCSEE) UNDER-THE-WING ENGINE COMPOSITE FAN BLADE DESIGN (General Electric Co.) 57 p HC A04/MF A01 CSCL 21E
N80-15113
Unclas
G3/07 33496

Prepared For

National Aeronautics and Space Administration

JAN 1980
RECEIVED
NASA STI FACILITY
ACCESS DEPT.

NASA Lewis Research Center
Contract NAS3-18021

TABLE OF CONTENTS

Section		Page
1.0	SUMMARY	1
2.0	DESIGN REQUIREMENTS	3
3.0	BASIC DESIGN FEATURES	6
	3.1 Fan Rotor Configuration	6
	3.2 Aerodynamic Design	6
	3.3 Blade Configuration	6
	3.4 Material Selection/Blade Layup Configuration	14
	3.5 Dovetail Design	20
	3.6 Platform Design	20
4.0	DESIGN ANALYSIS	26
	4.1 Blade Stress and Deflection Analysis	26
	4.2 Platform Stress and Vibration Analysis	32
	4.3 Blade Vibration Analysis	40
	4.4 Blade Impact Analysis	47
	4.5 Weight	47

PRECEDING PAGE BLANK NOT FILMED

LIST OF ILLUSTRATIONS

Figure		Page
1-1	QCSEE UTW Composite Fan Blade and Platform	2
3-1	UTW Experimental Engine	7
3-2	UTW Blade Geometry at Different Pitch Angle Settings	8
3-3	UTW Blade Chord Radial Distribution	10
3-4	UTW Blade Max Thickness Radial Distribution	10
3-5	UTW Blade Stagger Angle Radial Distribution	11
3-6	UTW Blade Camber Angle Radial Distribution	11
3-7	UTW Composite Fan Blade	12
3-8	Molded Fan Blade	13
3-9	Blade Airfoil Sections	15
3-10	Radial Sections Through the Molded Blade	16
3-11	Ply Layup and Material Arrangement	17
3-12	QCSEE UTW Composite Blade	19
3-13	Dovetail Molded Section	23
3-14	Platform Design	25
4-1	Finite Element Model - Composite Blade	27
4-2	UTW Blade Resultant Radial Stress	28
4-3	Calculated Blade Radial Stress	
4-4	Calculated Blade Chordal Stress	30
4-5	Calculated Blade Interlaminar Shear Stress	31
4-6	UTW Blade Displacements and Twist	33
4-7	Calculated Blade Relative Radial Stresses for First Flexural Mode	34

LIST OF ILLUSTRATIONS (Cont'd)

Figure		Page
4-8	Calculated Blade Relative Radial Stresses for Second Flexural Mode	35
4-9	Calculated Blade Relative Radial Stresses for First Torsional Mode	36
4-10	Allowable Stress Range Diagram - Blade Radial Stress	37
4-11	Allowable Stress Range Diagram - Dovetail Normal Stress	38
4-12	Allowable Stress Range Diagram - Dovetail Shear Stress	39
4-13	Platform Cross Section	41
4-14	Limit Cycle Boundaries	45
4-15	Campbell Diagram - UTW Composite Blade	46
4-16	UTW Blade Transferred Impact Energy for a 1.81 kg (4 lb.) Bird	48
4-17	UTW Composite Blade Predicted Gross Impact Capability	49
4-18	UTW Blade Impact Momentum for a .68 kg (1½ lb.) Bird	50

LIST OF TABLES

Table		Page
2-I	QCSEE UTW Engine Standard Day Duty Cycle	4
3-I	QCSEE UTW Composite Fan Blade Preliminary Design Summary	9
3-II	PR288/AS Prepreg Properties	21
3-III	Composite Material Properties	22
4-I	Platform Stresses and Margins of Safety	42
4-II	Platform Natural Frequencies	43
4-III	UTW Composite Blade Weight Summary	51

SECTION 1.0

SUMMARY

An Under-The-Wing (UTW) fan rotor will be built and tested as part of the NASA QCSEE Program. This fan employs 18 variable pitch composite fan blades that conform to the aerodynamic design described in the Under-The-Wing Fan Final Design Report. The composite fan blades will be manufactured from a hybrid composite combination of materials consisting of Kevlar-49, type AS graphite, boron, and S-glass fibers in a PR288 epoxy resin matrix. The material is procured in prepregged ply form and molded under controlled pressure and temperature conditions to a final molded form. Erosion protection of the basic organic composite-material blade consists of nickel plating on stainless steel wire mesh which is bonded onto the molded blade and is applied to the leading edge portion of the blade. Polyurethane coating is applied over the remaining exposed composite material surfaces to provide erosion protection. A circular shaped platform that provides a portion of the inner flowpath wall is bonded directly to the blade. A model of the blade with attached platform is shown in Figure 1-1.

The blade has been designed for the experimental engine and will satisfy aerostability, lightweight, cyclic life and strength requirements with the margins identified in Section 4.0, Design Analysis. A further modification of the blade, based on more recent developments in foreign object damage resistance, is planned for subsequent flight-type hardware.

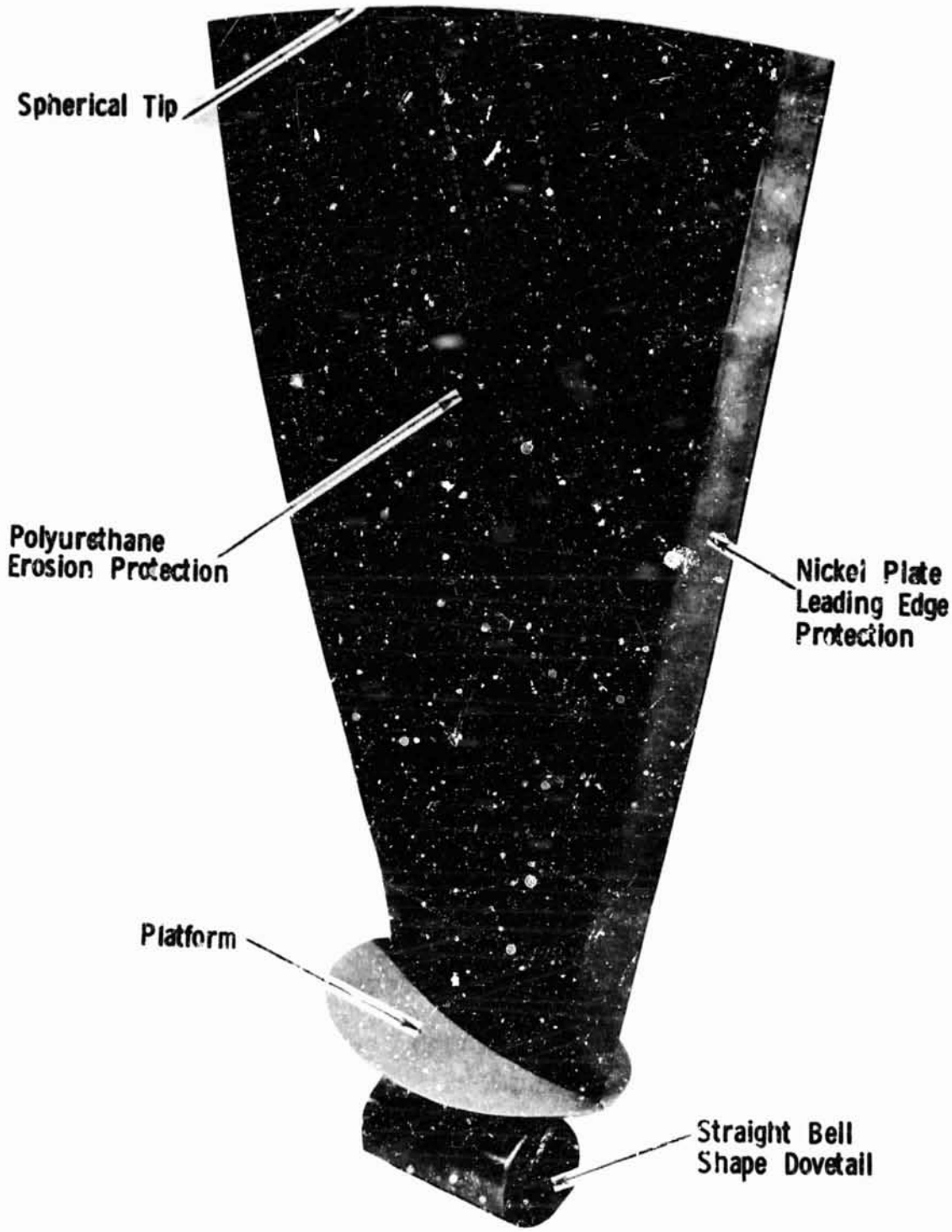

Figure 1-1. QCSEE UTW Composite Fan Blade and Platform.

ORIGINAL PAGE IS
OF POOR QUALITY

SECTION 2.0

DESIGN REQUIREMENTS

The design requirements for the UTW composite fan blade were established to provide realistic long life operation of a flight engine based on the standard day duty cycle shown in Table 2-I. The design requirements are listed as follows:

- Design Mechanical Speeds
  - 100% mechanical design - 3244 rpm
  - 100% SLS hot day takeoff - 3143 rpm
  - Maximum steady-state duty cycle speed - 3326 rpm
  - Maximum design overspeed - 3614 rpm
  - Maximum burst speed - 4700 rpm
- Design Life and Cycles
  - 36,000 hours
  - 48,000 cycles
  - 1,000 ground check-out cycles, full power
- Mechanical Design Requirements
  - Blade is capable of operation in reverse thrust traversing to reverse through flat pitch or through stall pitch.
  - Blades are individually replaceable without major teardown.
  - Blade untwist has been factored into airfoil configuration.
  - Stresses are within allowable stress range diagram, with sufficient vibratory margin.
  - First flexural frequency crosses 2/rev above flight idle and below takeoff and climb engine speeds.
  - First flexural frequency has greater than 15% margin over 1/rev at 115% speed.
  - Blade nickel leading edge protection has been kept within aero airfoil limits.

Table 2-I. QCSEE UTW Engine Standard Day Duty Cycle.

Segment	Altitude (km)	Mach Number	% Thrust	Time (Minutes)	Time (%)	Fan Speed (rpm)
Start	0	0	-	0.5	1.1	0 - 902
Idle/Taxi	0	0	3 - 15	3.1	6.9	902
Takeoff	0	0	100***	1.22	2.7	3157
Climb - 1	0 - 3	0.38 - 0.43	100	5.0	11.1	2934 - 3105
Climb - 2	3 - 7.6	0.53 - 0.70	100	5.0	11.1	3107 - 3341
Cruise	7.6	0.70	70 - 85	14.0	31.1	2912 - 3074
Descent	0.3 - 6	0.60	15	11.7	26.0	1972 - 2051
Approach	0 - 0.3	0.12	65	1.3	2.9	3090
Reverse	0	0 - 0.12	Max. Rev.***	0.08	0.2	2977** - 3408*
Idle/Taxi	0	0	3 - 15	3.1	6.9	0 - 902
				45.0	100.0	

* Thru Flat Pitch
** Thru Stall
*** +31° Day

Of these mechanical design requirements, the first is of prime importance. Successful operation of the experimental engine hinges to a great degree on having a blade which can withstand reverse-pitch operation and other inlet disturbances including crosswind testing. Initially the design requirements included provisions for satisfying FAA specifications for FOD resistance. However, during the testing of preliminary blades it was found that the blade FOD capability was deficient and FOD requirements were dropped pending further developments on other NASA and related programs.

SECTION 3.0

BASIC DESIGN FEATURES

3.1 FAN ROTOR CONFIGURATION

A cross section of the UTW experimental engine showing the fan configuration is presented in Figure 3-1. There are 18 variable-pitch composite rotor blades. The root of each blade is attached to a rotor trunnion. The trunnions are retained by the disk. Retainer straps, attached to the trunnion, lock the blade in axial position and resist trunnion opening deflections under blade centrifugal loading. A slot located in the outer casing at the rotor tip permits individual blade removal in the engine. After removal of the forward retainer strap the blade can be pulled directly forward out of the trunnion slot.

The solidity of the blade airfoil is 0.95 at the blade tip and 0.98 at the hub, thus the blades can rotate about their axis without touching the adjacent blade. The chord length is linear with radius. This permits rotation of the blades into the reverse thrust mode of operation through either the flat-pitch and the stall-pitch directions. Figure 3-2 shows a tip and a hub section of two adjacent blades in the nominal-pitch position, the reverse through stall pitch position and the reverse through flat pitch position. The spherical casing radius and the spherical blade tip provide good blade tip clearance throughout the range of blade pitch-angle settings. Circumferential grooved casing treatment is incorporated over the rotor tip to improve stall margin. An additional benefit of the casing treatment is to reduce the material bulk over the blade tip, for a given clearance, which will reduce the severity of an inadvertent blade rub.

3.2 AERODYNAMIC BLADE PARAMETERS

A summary of the aero blade parameters is presented in Table 3-I. The blade chord, maximum thickness, stagger angle and camber are plotted as a function of blade span in Figures 3-3, 3-4, 3-5 and 3-6 respectively.

3.3 BLADE CONFIGURATION

The finished blade configuration is shown in Figure 3-7 and consists of a molded composite blade and a molded composite platform. The molded blade is shown in Figure 3-8. The platform is described in Section 3.6, Platform Design.

The blade molded configuration consists of a solid composite airfoil and a straight bell-shaped composite dovetail. The molded blade leading edge is slightly reduced in thickness along the entire span to allow space for nickel

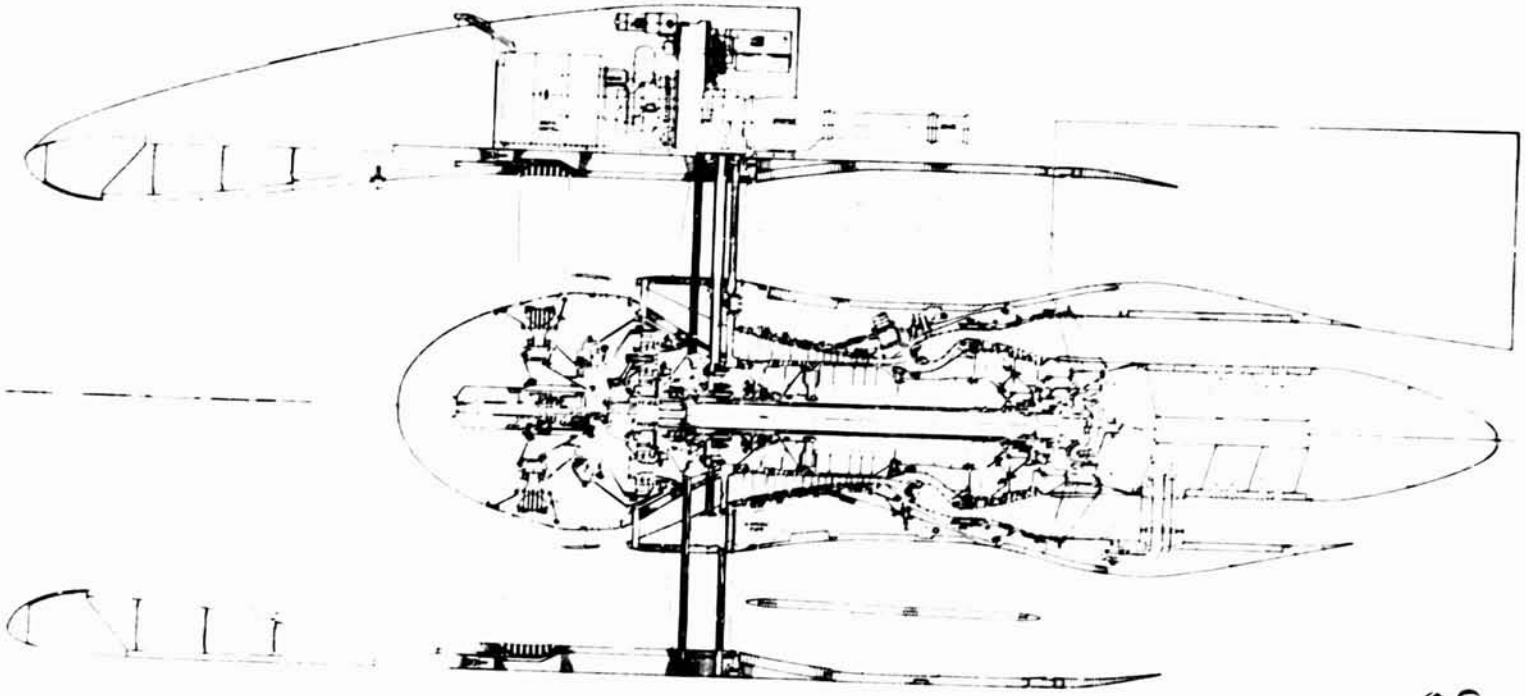

Figure 3-1. UTW Experimental Engine.

ORIGINAL PAGE IS
OF POOR QUALITY

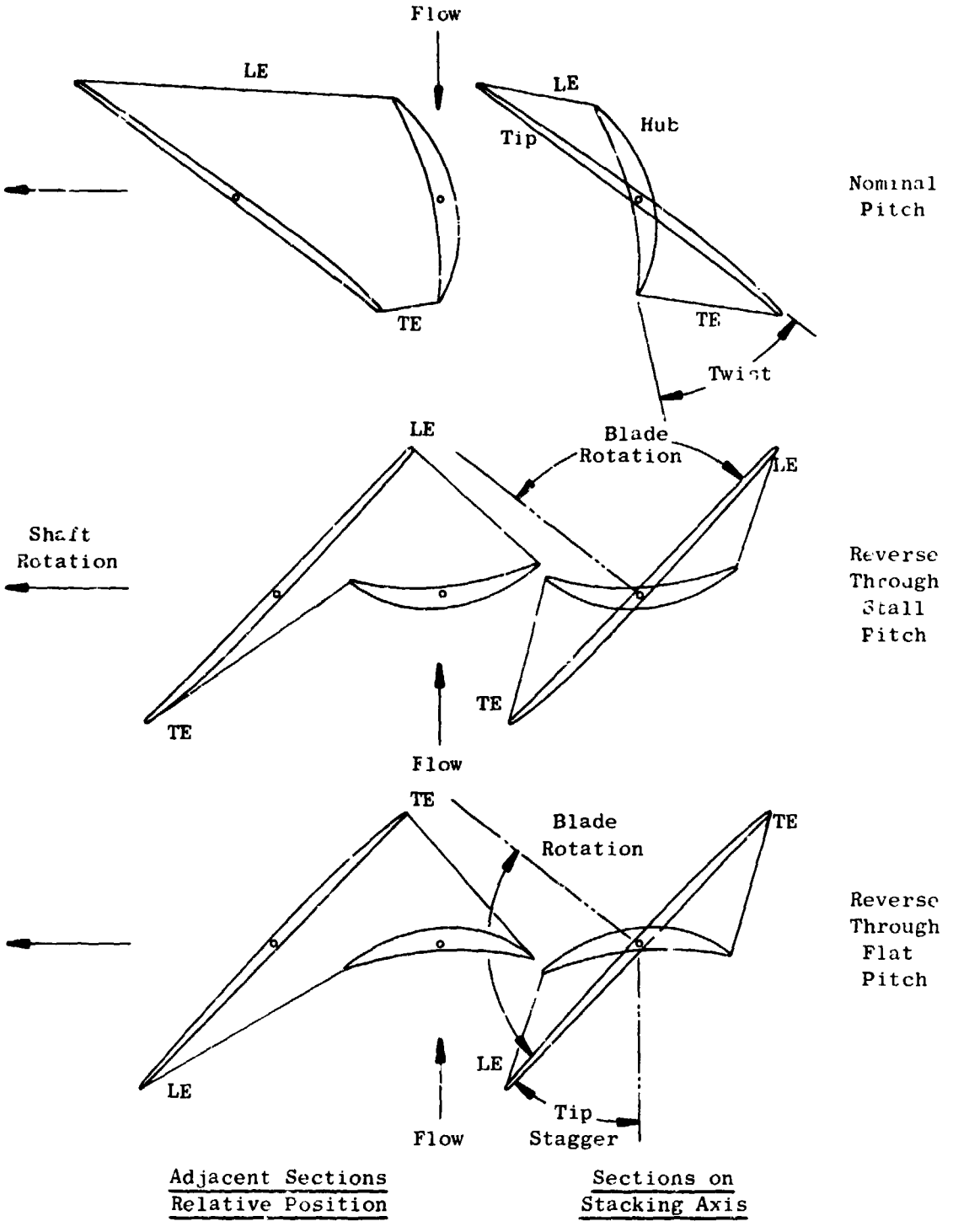

Figure 3-2. UTW Blade Geometry at Different Pitch Angle Settings.

Table 3-I. QCSEE UTW Composite Fan Blade Design Summary.

Aero Definition	
Tip Speed	306 m/sec (1005 ft/sec)
Tip Diameter	180 cm (71 in.)
Radius Ratio	0.44
Number of Blades	18
Bypass Pressure Ratio	1.27 Takeoff
Aspect Ratio	2.11
Tip Chord	30.3 cm (11.91 in.)
Root Chord	14.8 cm (5.82 in.)
T_M Root	1.92 cm (0.76 in.)
T_M Tip	0.91 cm (0.36 in.)
Root Camber	66.2°
Total Twist	45°
Solidity	
Tip	0.95
Root	0.98
Angle Change from Forward to Reverse	
Through Flat Pitch	75%
Through Stall	100%

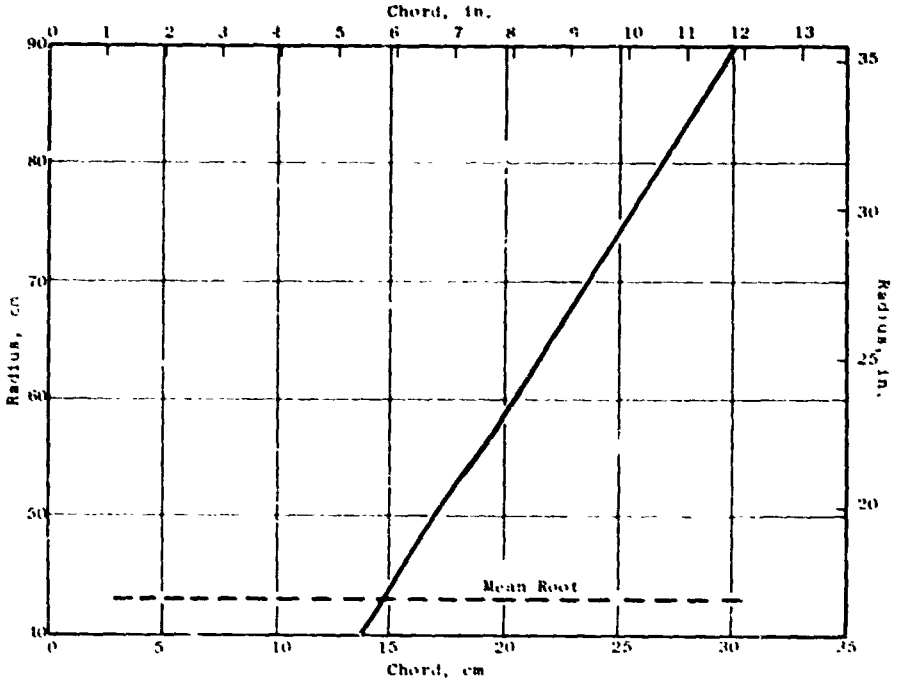

Figure 3-3. UTW Blade Chord Radial Distribution.

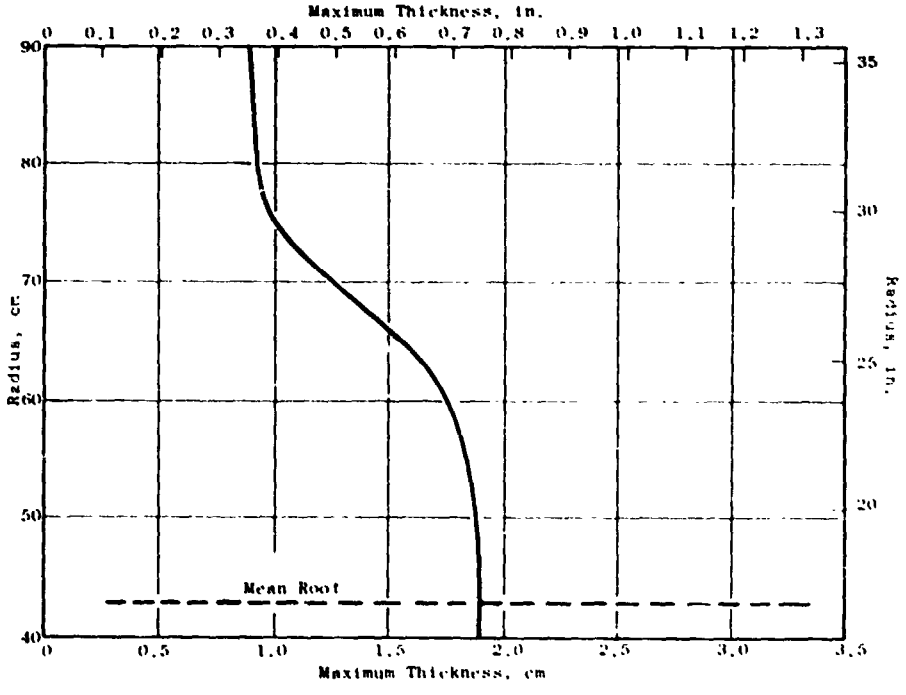

Figure 3-4. UTW Blade Max. Thickness Radial Distribution.

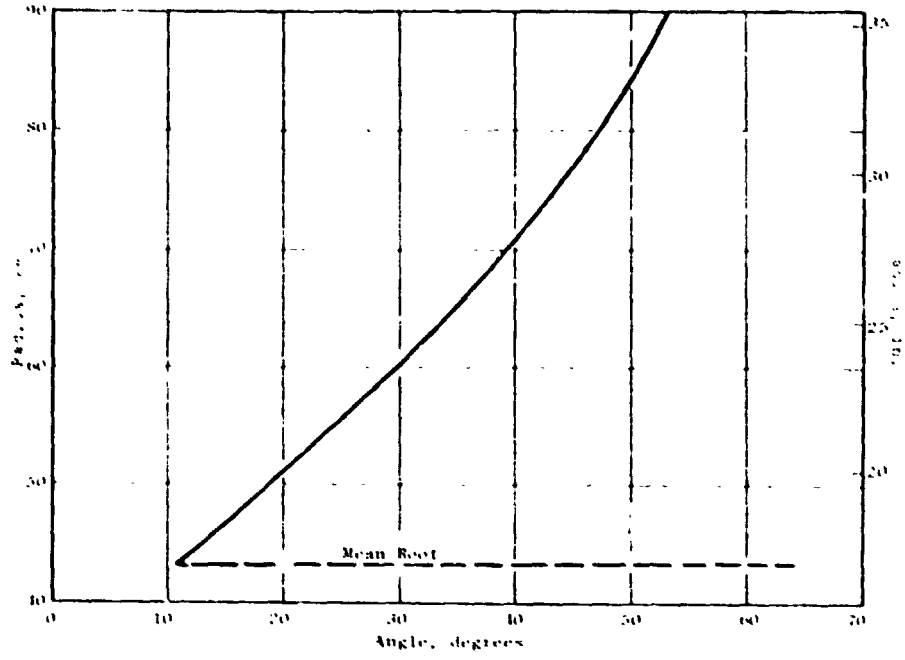

Figure 3-5. UTW Blade Stagger Angle Radial Distribution.

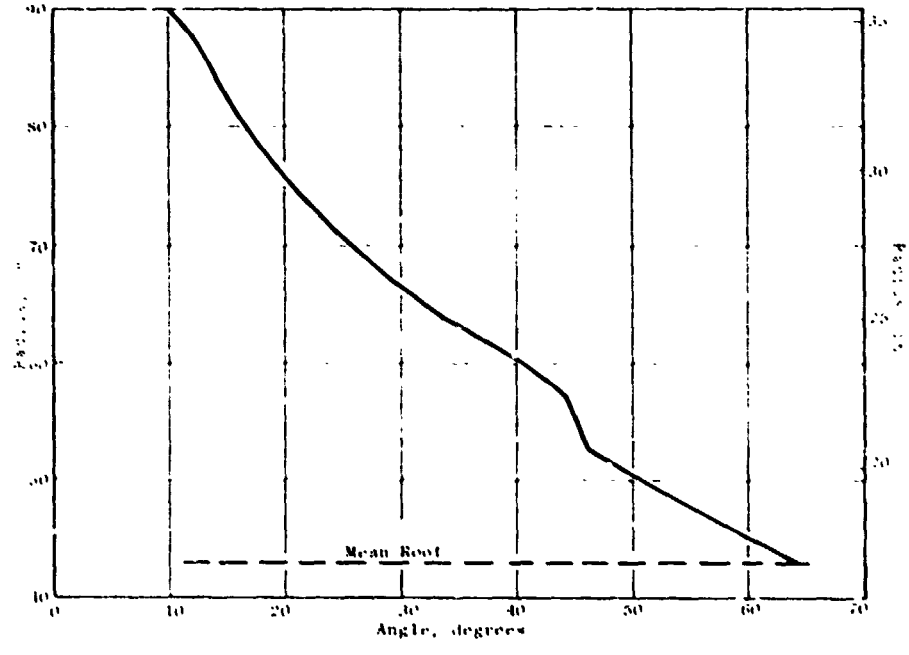

Figure 3-6. UTW Blade Camber Angle Distribution.

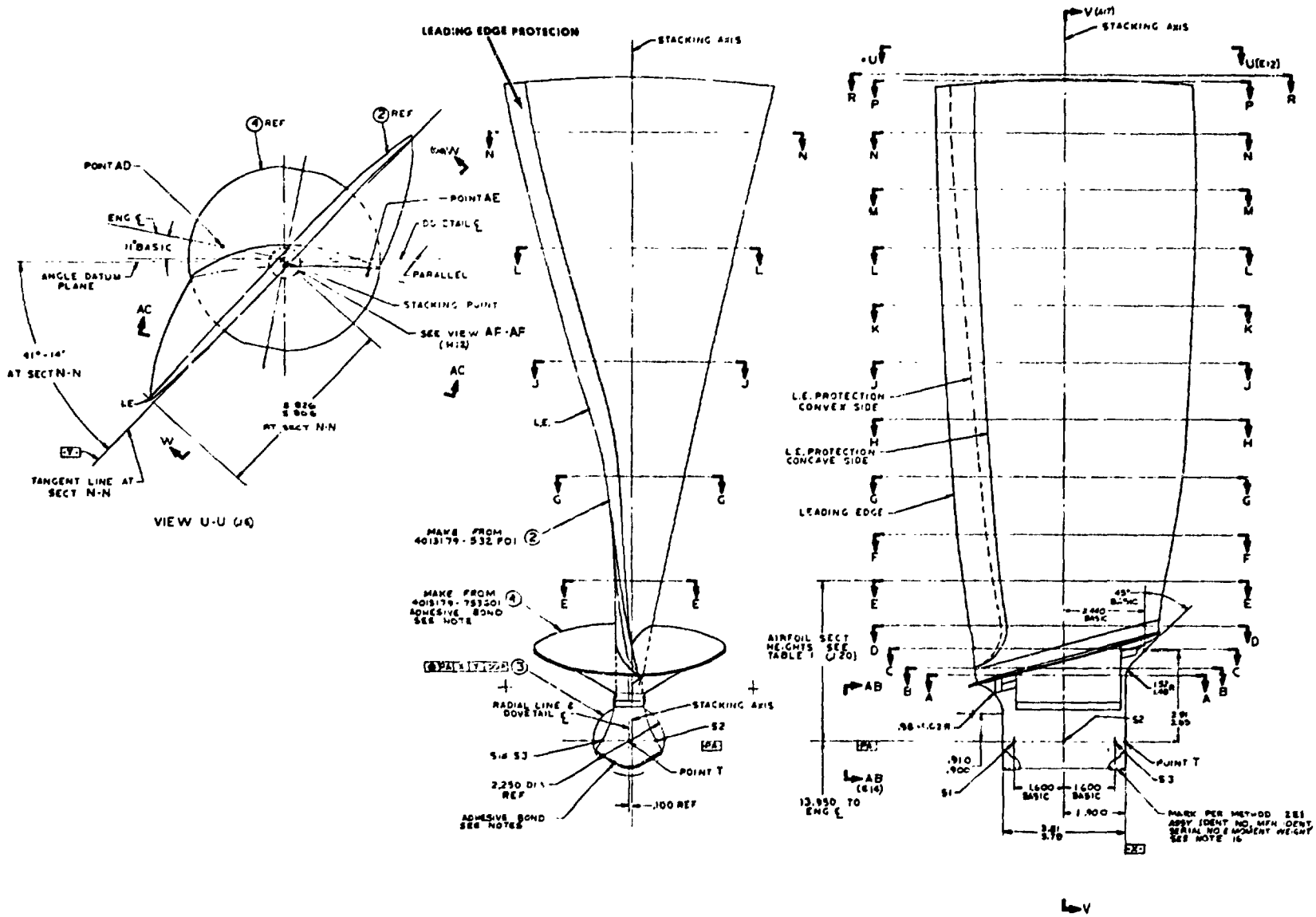

Figure 3-7. UTW Composite Fan Blade.

ORIGINAL PAGE IS
OF POOR QUALITY

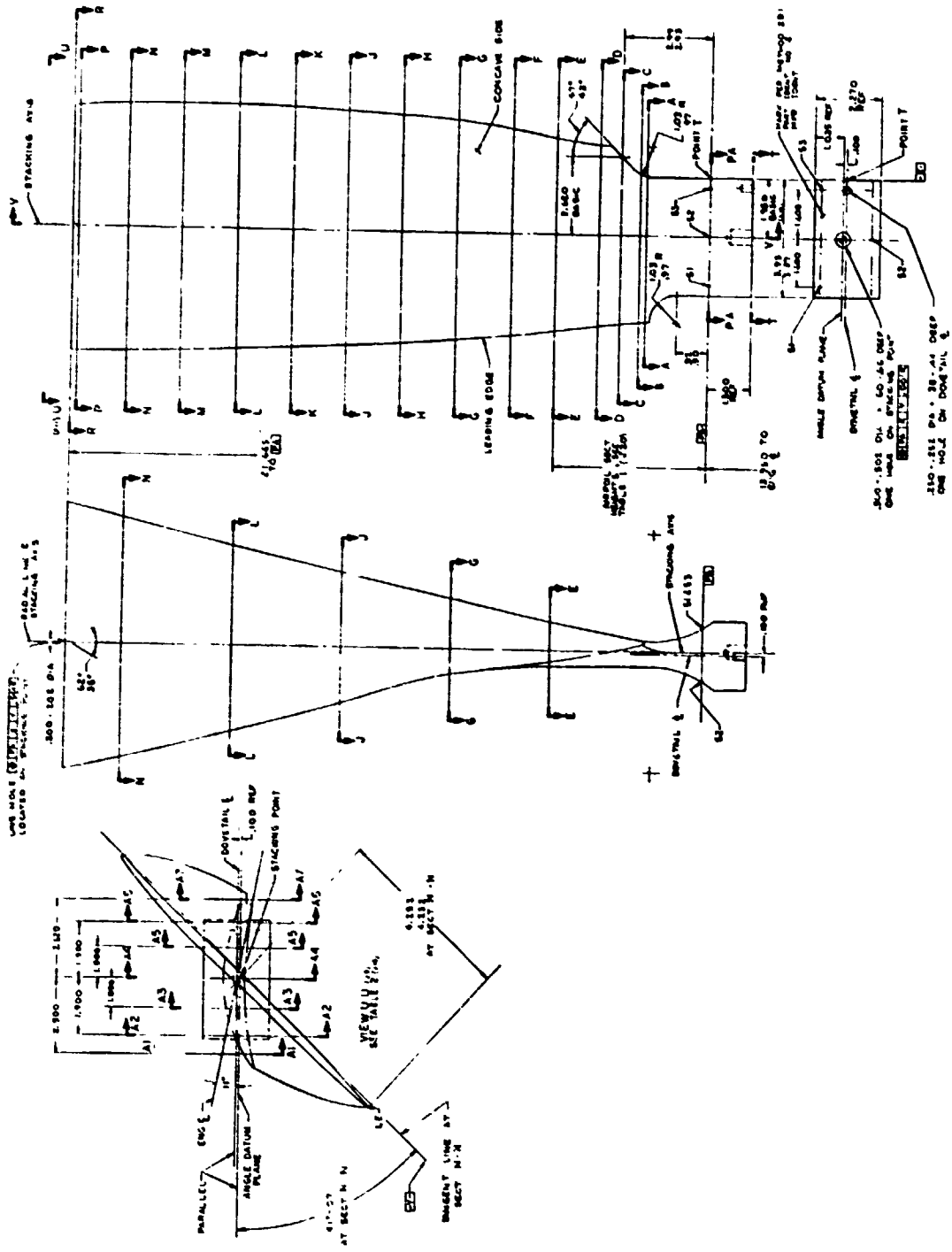

Figure 3-8. Molded Fan Blade.

plate over wire mesh protection within the final aero configuration. The dovetail is undercut at the leading edge and trailing edge to permit better transitioning of the cambered airfoil section into the straight dovetail and match the rotor trunnion configuration.

The airfoil definition is described by 15 radially spaced airfoil cross sections which are stacked on a common axis. These are shown along with details of the blade cross sections in Figure 3-9. Each section location corresponds to the like designated elevation defined on the blade, Figure 3-7. The dotted portion of the leading edge defines the aero profile and the solid inner portion describes the molded composite cross section. Only a portion of the lowest three sections extend above the flowpath. The aft portion of these sections lie below the platform, therefore they do not need to correspond with aero defined profiles.

Radial sections through the molded blade are shown in Figure 3-10. The dovetail axial centerline is offset from the stacking axis by 0.254 cm (0.1 in.) to provide a smooth airfoil-to-dovetail transition.

3.4 MATERIAL SELECTION/BLADE LAYUP CONFIGURATION

The material selection and ply arrangement for the UTW hybrid composite blade is based on previous development efforts conducted by General Electric and sponsored by NASA under Contract NAS3-16777, Impact Resistance of Composite Fan Blades, and development effort conducted during the preliminary design phase of the QCSEE Program. These efforts led to the selection of a combination of fibers in a single blade to provide the proper frequency responses to satisfy STOL engine conditions. Figure 3-11 shows the general ply shapes, layup arrangement, fiber orientations and material in each ply of the blade. Figure 3-12 shows a trimetric view of the general arrangement of the plies in the blade. The flex root surface plies in the lower region of the blade contain S-glass fibers. These plies being near the surface and having relatively low bending stiffness and high tensile strength provide higher strain-to-failure characteristics thereby allowing the blade to absorb large bird impact loading without the root failure that usually accompanies brittle composite materials. Torsional stiffening plies in the airfoil region of the blade are oriented at $\pm$ 45° to provide the shear modulus required for a high first torsional frequency. These plies contain boron towards the outer surfaces of the blade and graphite in the inner regions. Plies of Kevlar-49 are interspersed throughout the blade with the majority of them being oriented with their fibers in the longitudinal direction of the blade. Several Kevlar-49 plies in the tip region of the blade are oriented at 90° to the longitudinal axis to provide chordwise strength and stiffness to the blade.

The resin system being used in this program is a product of the 3M Company and is designated as PR288. This is a resin system that has proven satisfactory for the needs of advanced composite blading. Some of its unique characteristics in the prepreg form are:

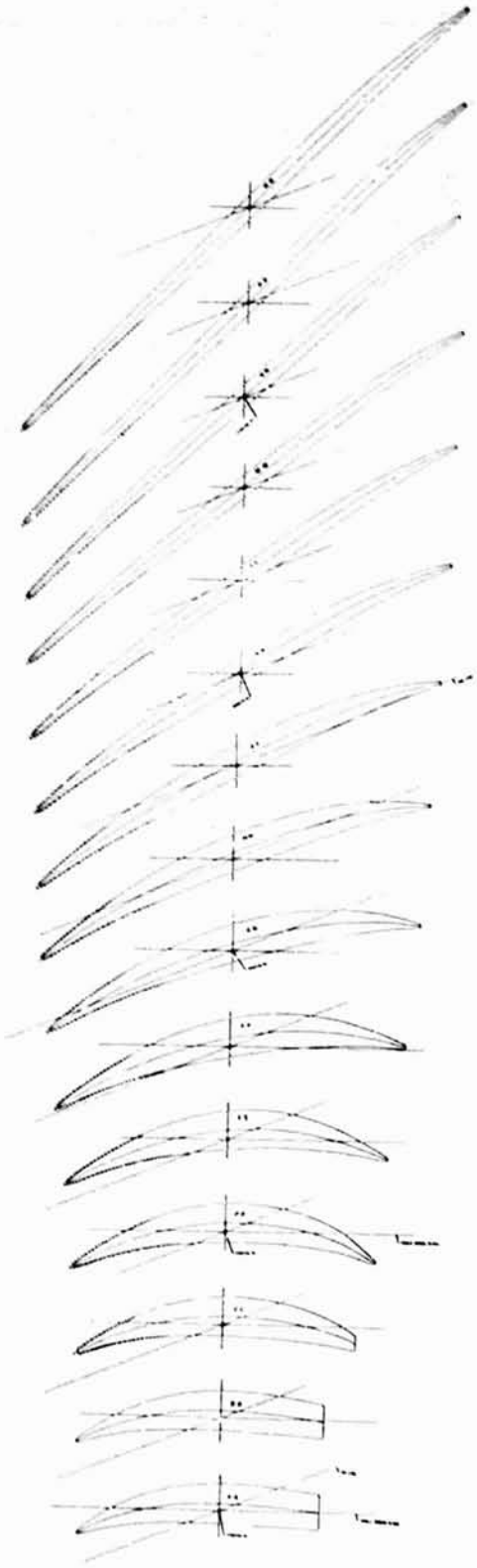

Figure 3-9. Blade Airfoil Sections.

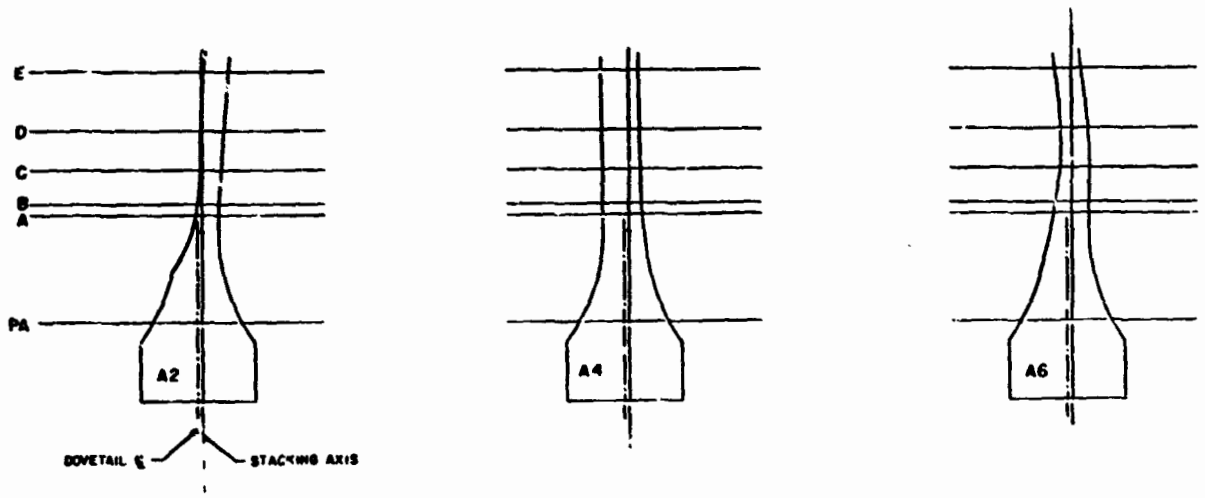

Forward Face of Dovetail

Midchord

Aft Face of Dovetail

Figure 3-10. Radial Sections Through the Molded Blade.

ORIGI
OF P

FOLDOUT FRAME 1

PLY NO.	PLY ORIENT ANGLE AIRFOIL	PLY ORIENT ANGLE INSERT	MATERIAL
1	—	+45°	SG
2	—	-45°	B
3	—	+45°	B
4	—	-45°	B
5	—	0°	B
6	—	0°	B
7	—	0°	B
8	+45°	—	SG
9	+45°	—	B
10	0°	—	SG
11	0°	—	SG
12	—	-45°	B
13	—	-45°	B
14	—	0°	GR
15	—	-45°	GR
16	+45°	—	SG
17	0°	—	GR
18	—	+45°	GR
19	—	0°	GR
20	—	-45°	GR
21	0°	—	SG
22	—	+45°	GR
23	—	0°	GR
24	+45°	—	B
25	—	0°	GR
26	—	-45°	GR
27	0°	—	GR
28	—	+45°	GR
29	—	0°	GR
30	—	+45°	GR
31	—	0°	GR
32	—	-45°	GR
33	0°	—	K
34	—	+45°	SG
35	—	0°	GR
36	+45°	—	GR
37	—	0°	GR
38	—	-45°	GR
39	0°	—	K
40	—	+45°	GR
41	—	0°	GR
42	-45°	—	GR
43	—	0°	GR
44	—	-45°	GR
45	0°	—	K
46	—	+45°	GR
47	—	0°	GR
48	+45°	—	GR
49	—	0°	GR
50	—	-45°	GR
51	0°	—	GR
52	—	+45°	GR
53	—	0°	GR
54	-45°	—	GR
55	—	0°	GR
56	—	-45°	GR
57	0°	—	K
58	—	+45°	GR
59	—	0°	GR
60	+45°	—	GR
61	—	0°	GR
62	—	-45°	GR
63	0°	—	K
64	—	+45°	GR
65	—	0°	GR
66	-45°	—	GR
67	—	0°	GR
68	—	+45°	GR
69	0°	—	GR
70	—	0°	GR
71	+45°	—	GR
72	—	0°	GR
73	—	-45°	GR
74	0° *	—	K
75	—	+45°	GR
76	—	0°	GR
77	-45°	—	GR
78	—	0°	GR
79	—	-45°	GR
80	0°	—	K
81	—	+45°	GR
82	—	0°	GR
83	+45°	—	GR
84	—	0°	GR
85	—	-45°	GR
86	0° *	—	K
87	—	+45°	GR
88	—	0°	GR
89	-45°	—	GR
90	—	0°	GR
91	—	-45°	GR
92	0°	—	K
93	—	-45°	GR

* CONTAINS 90° PLIES IN TIP REGION

PLY NO.	PLY ORIENT ANGLE AIRFOIL	PLY ORIENT ANGLE INSERT	MATERIAL
94	—	0°	GR
95	+45°	—	GR
96	—	+45°	GR
97	0°	—	GR
98	—	-45°	GR
99	—	0°	GR
100	—	0°	GR
101	0° *	—	K
102	—	+45°	GR
103	—	0°	GR
104	—	-45°	GR
105	-45°	—	GR
106	—	0°	GR
107	—	+45°	GR
108	—	0°	GR
109	0°	—	K
110	—	-45°	GR
111	—	0°	GR
112	—	+45°	GR
113	—	0°	GR
114	0°	—	K
114A	0°	—	GR
115A	0°	—	GR
115	0°	—	K
116	—	0°	GR
117	—	+45°	GR
118	—	0°	GR
119	—	-45°	GR
120	0°	—	K
121	—	0°	GR
122	—	+45°	GR
123	—	0°	GR
124	-45°	—	GR
125	—	-45°	GR
126	—	0°	GR
127	—	+45°	GR
128	0° *	—	K
129	—	0°	GR
130	—	-45°	GR
131	—	0°	GR
132	+45°	—	GR
133	—	+45°	GR
134	—	0°	GR
135	—	-45°	GR
136	0°	—	K
137	—	-45°	GR
138	—	0°	GR
139	-45°	—	GR
140	—	0°	GR
141	—	+45°	GR
142	0° *	—	K
143	—	-45°	GR
144	—	0°	GR
145	+45°	—	GR
146	—	0°	GR
147	—	+45°	GR
148	0°	—	K
149	—	-45°	GR
150	—	0°	GR
151	-45°	—	GR
152	—	0°	GR
153	—	+45°	GR
154	0° *	—	K
155	—	-45°	GR
156	—	0°	GR
157	+45°	—	GR
158	—	0°	GR
159	—	+45°	GR
160	0°	—	K
161	—	-45°	GR
162	—	0°	GR
163	-45°	—	GR
164	—	0°	GR
165	—	+45°	GR
166	0°	—	K
167	—	-45°	GR
168	—	0°	GR
169	+45°	—	GR
170	—	0°	GR
171	—	+45°	GR
172	0°	—	K
173	—	-45°	GR
174	—	0°	GR
175	-45°	—	GR
176	—	0°	GR
177	—	+45°	GR
178	0°	—	K
179	—	-45°	GR
180	—	0°	GR
181	+45°	—	GR
182	—	0°	GR
183	—	+45°	GR
184	0°	—	K
185	—	-45°	GR
186	—	0°	GR
187	-45°	—	GR
188	—	0°	GR
189	—	+45°	GR
190	0°	—	K
191	—	-45°	GR
192	—	0°	GR

PLY NO.	PLY ORIENT ANGLE AIRFOIL	PLY ORIENT ANGLE INSERT	MATERIAL
193	+45°	—	GR
194	—	0°	GR
195	—	+45°	GR
196	0°	—	GR
197	—	-45°	GR
198	—	0°	GR
199	-45°	—	GR
200	—	0°	GR
201	—	+45°	GR
202	0°	—	SG
203	—	-45°	GR
204	—	0°	GR
205	+45°	—	B
206	—	0°	GR
207	—	+45°	GR
208	0°	—	SG
209	—	-45°	GR
210	—	0°	GR
211	-45°	—	B
212	—	0°	GR
213	—	+45°	TH
214	0°	—	SG
215	—	-45°	GR
216	—	0°	GR
217	+45°	—	B
218	—	0°	GR
219	—	+45°	GR
220	0°	—	SG
221	—	-45°	GR
222	—	0°	GR
223B	-45°	—	B
223A	-45°	—	B
224	0°	—	SG
225	0°	—	SG
226B	+45°	—	B
226A	+45°	—	B
227	0°	—	SG
228	0°	—	
K	—	-45°	
K	—	+45°	
K	—	-45°	
K	—	+45°	
K	—	+45°	SG

Figure 3-11. Ply Layup

ORIGINAL PAGE IS
OF POOR QUALITY

FOLDOUT FRAME 2

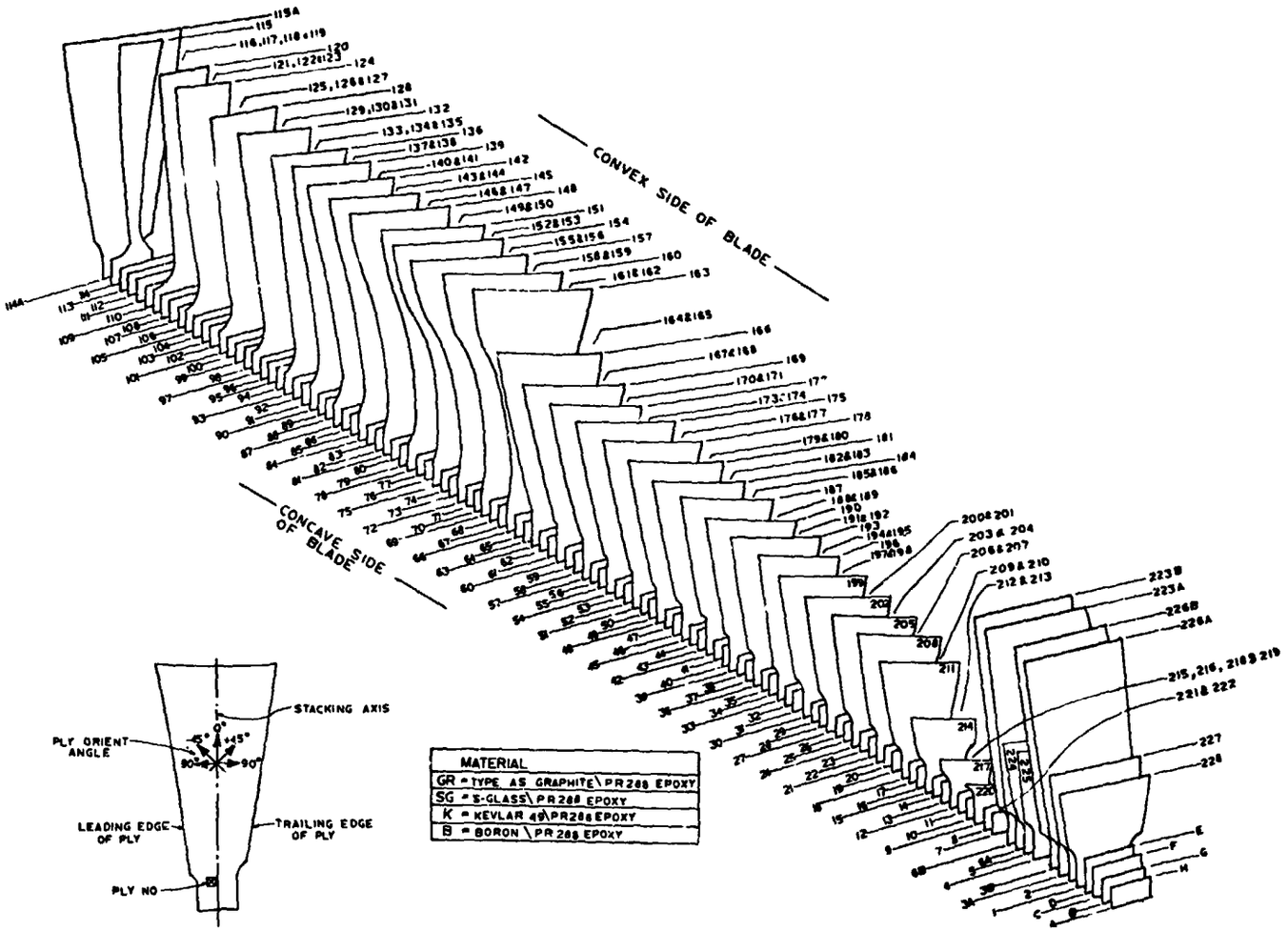

11. Ply Layup and Material Arrangement.

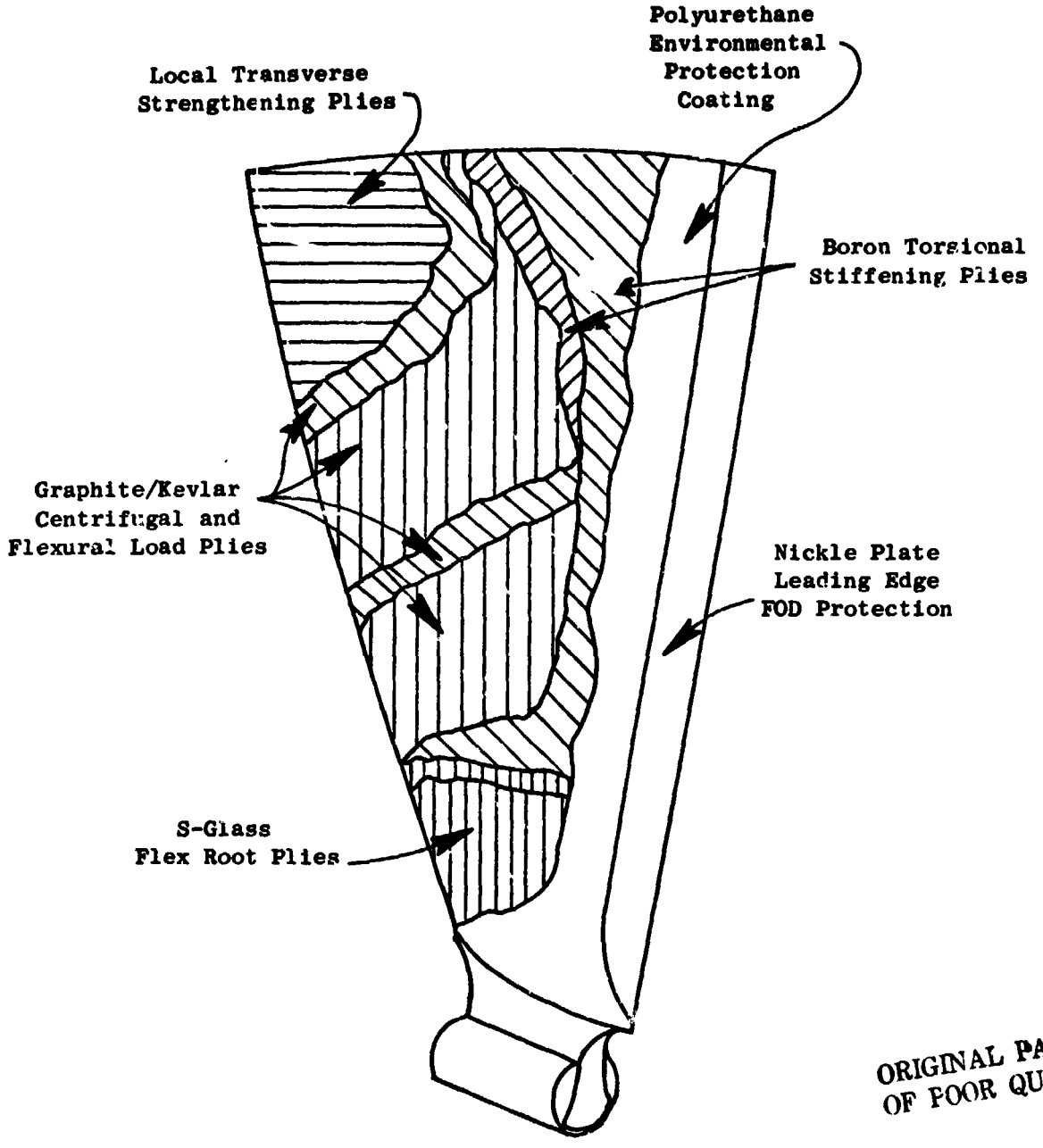

ORIGINAL PAGE IS
OF POOR QUALITY

Figure 3-12. QCSEE UTW Composite Blade.

PRECEDING PAGE BLANK NOT FILMED

- Has consistent processing characteristics.
- Can be prepregged with many different fibers including hybrids.
- Uniform prepreg thickness and resin content control.

Typical processing shedules and properties of the PR288/AS prepreg are shown in Table 3-II. Material properties for the various fiber composite prepregs used are shown in Table 3-III.

3.5 DOVETAIL DESIGN

The dovetail design for the composite blade consists of a straight bell-shaped dovetail with a 8.89 cm (3-1/2 in.) radius. The bell shaped dovetail design achieves an efficient configuration having both high static pull strength and good fatigue strength. All airfoil plies extend continuously down into the dovetail and are interspersed with insert plies which act to fill out the enlarged cross section. This is seen in Figure 3-13 which shows a radial section of the blade root and dovetail prior to dovetail machining.

3.6 PLATFORM DESIGN

The QCSEE UTW engine incorporates a variable pitch fan. The blade variable pitch operation requires a circular opening through the spinner and hub to permit airfoil clearance in the different blade position rotations - either actuated in the flat pitch or stall direction. To maintain reasonable actuation forces and blade dovetail stresses, the centrifugal loading on each blade platform and dovetail is required to be kept to a minimum. This requires a lightweight design. Therefore, composite platforms in addition to composite blades are necessary. The following paragraphs summarize the design requirements and description of the platform. The stress and vibration analysis results are tabulated and the weight and fabrication process is described in Section 4.2, Platform Stress and Vibration Analysis.

The platform design selected for the QCSEE UTW blade satisfies several requirements including (1) lightweight - less than 0.16 kg (0.35 lb.), (2) a structural stress margin of safety of 2 at 3326 rpm to provide for positive margin at the design burst condition of 4700 rpm, (3) a fail safe design in the event the platform to blade bond becomes ineffective, and (4) a low radial deflection - less than 0.05 cm (0.020 in.) at tip of platform overhang. In addition, the circular opening required for blade rotation is filled by the platform. The platform is attached to the blade and contoured to match closely the spinner and hub which make up the fan inner aerodynamic contours and provide a smooth inner flowpath. The platform is also designed to avoid interference with adjacent blades and adjacent platforms during variable pitch blade turning.

Structurally the platform is a varying width tapered beam cantilevered from the blade root. It consists of honeycomb core stabilized by upper and

Table 3-II - PR288/AS Prepreg Properties

Property	PR288/AS
Supplier	3M
Process	Film - Cont. Tape
Cure Schedule	2.5 hrs. at 129° C (265° F)
Postcure Schedule	4 hrs at 135° C (275° F)
Flexural Strength	
Room Temperature	193 kN/cm^2 (280 ksi)
121° C(250° F)	138 kN/cm^2 (200 ksi)
Elastic Mod.	
Room Temperature	11.9 kN/cm^2 (17.2 ksi)
121° C(250° F)	11.6 kN/cm^2 (16.8 ksi)
Short Beam Shear	
Room Temperature	9.0 kN/cm^2 (13.0 ksi)
121° C(250° F)	5.2 kN/cm^2 (7.5 ksi)
Charpy Impact	8.0 m-N (6.0 ft-lb)
Fiber Volume, %	59.8
Sp. Gr., g/cc	1.58
Void Content, %	0.0

Table 3-III. Composite Material Properties.

	PR288 AS Graphite	PR288 Boron	PR288 S-Glass	PR288 Kevlar 49
Fiber Volume, Percent	60	55	60	60
Elastic Modulus, $10^6 N/cm^2$ (10^6 psi) (0° Orientation)	11.9 (17.2)	20.0 (29.0)	5.9 (8.5)	7.6 (11.0)
Elastic Modulus, $10^6 N/cm^2$ (10^6 psi) (90° Orientation)	1.1 (1.6)	1.2 (1.8)	0.8 (1.1)	0.6 (0.8)
Elastic Modulus, $10^6 N/cm^2$ (10^6 psi) (0/22/0/-22 Orientation)	9.5 (13.8)	11.7 (17.0)	4.7 (6.8)	5.9 (8.6)
Shear Modulus, $10^6 N/cm^2$ (10^6 psi) (0/22/0/-22)	1.1 (1.6)	1.9 (2.7)	0.6 (0.9)	0.6 (0.93)
Density, G/cm^3 (lb/in^3)	1.5 (0.056)	1.9 (0.070)	2.0 (0.072)	1.4 (0.050)
Tensile Strength, kN/cm^2 (ksi) (0°)	138 (200)	138 (200)	138+ (200+)	138 (200)
Tensile Strength, kN/cm^2 (ksi) (0/22/0/-22)	95 (138)	95 (138)	95+ (138+)	95 (138)
Flex Strength, kN/cm^2 (ksi) (0°)	193 (280)	---	---	62 (90)
Flex Strength, kN/cm^2 (ksi) (0/22/0/-22)	168 (244)	---	172 (250)	59 (85)
Shear Strength, kN/cm^2 (ksi) (0°)	9.0 (13.0)	7.6 (11.0)	8.1 (11.8)	3.4-7 (5-10)
Charpy Impact, m-N (ft-lb) (±10°)	8 (6)	10 (7.5)	47 (35)	23 (17)

ORIGINAL PAGE IS
OF POOR QUALITY

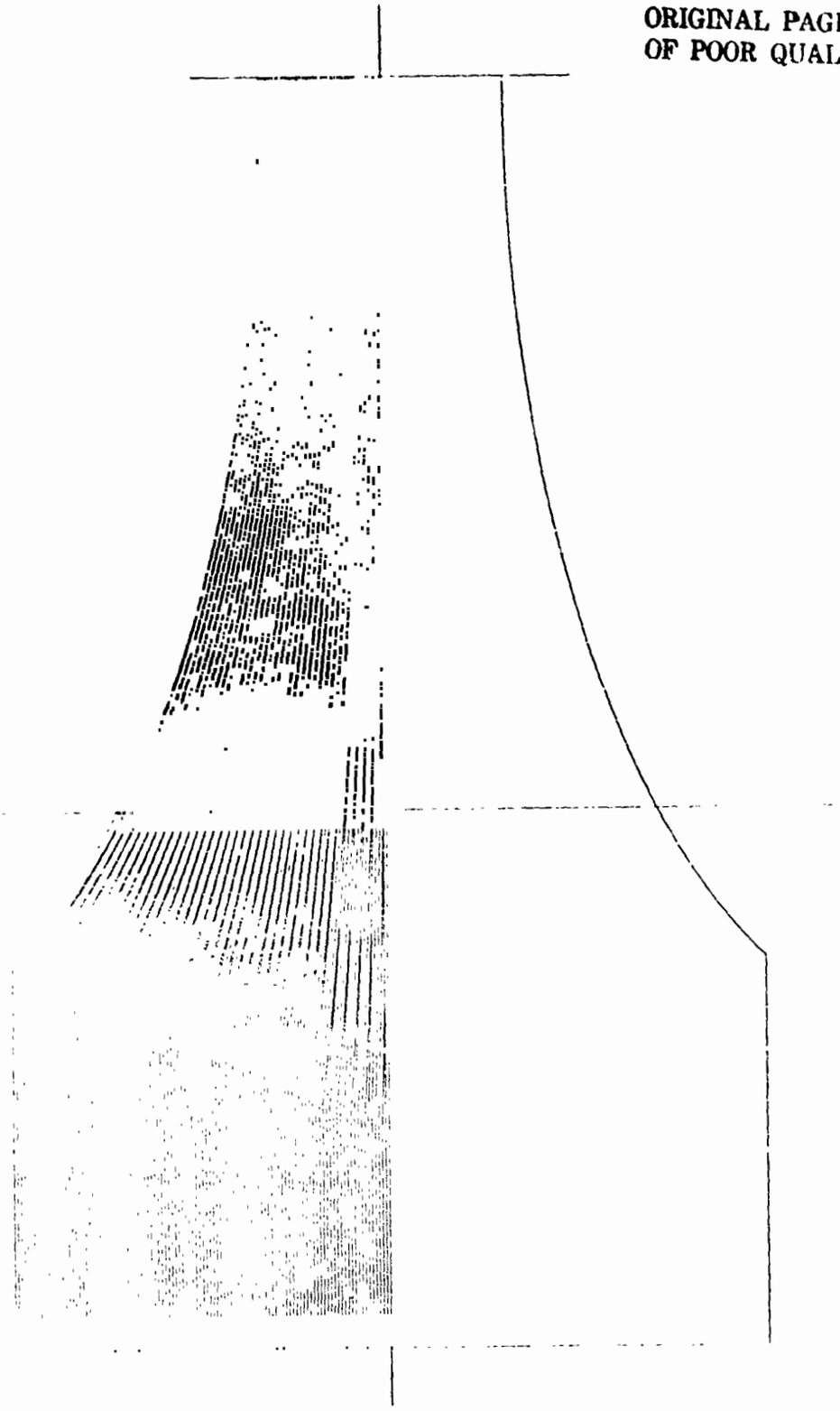

Figure 3-13. Dovetail Molded Section.

lower graphite/epoxy face sheets which are simultaneously molded and bonded onto the blade using a co-curing process. The result is a one piece platform design. With structural plies extending around the blade root leading and trailing edge undercuts, the single piece deisgn has the inherent capability of being retained even with a complete loss of the blade-to-platform adhesive bond. This satisfies the fail safe requirements.

Figure 1-1 shows a typical platform on the blade, while Figure 3-14 is a schematic showing the platform details.

ORIGINAL PAGE IS
OF POOR QUALITY

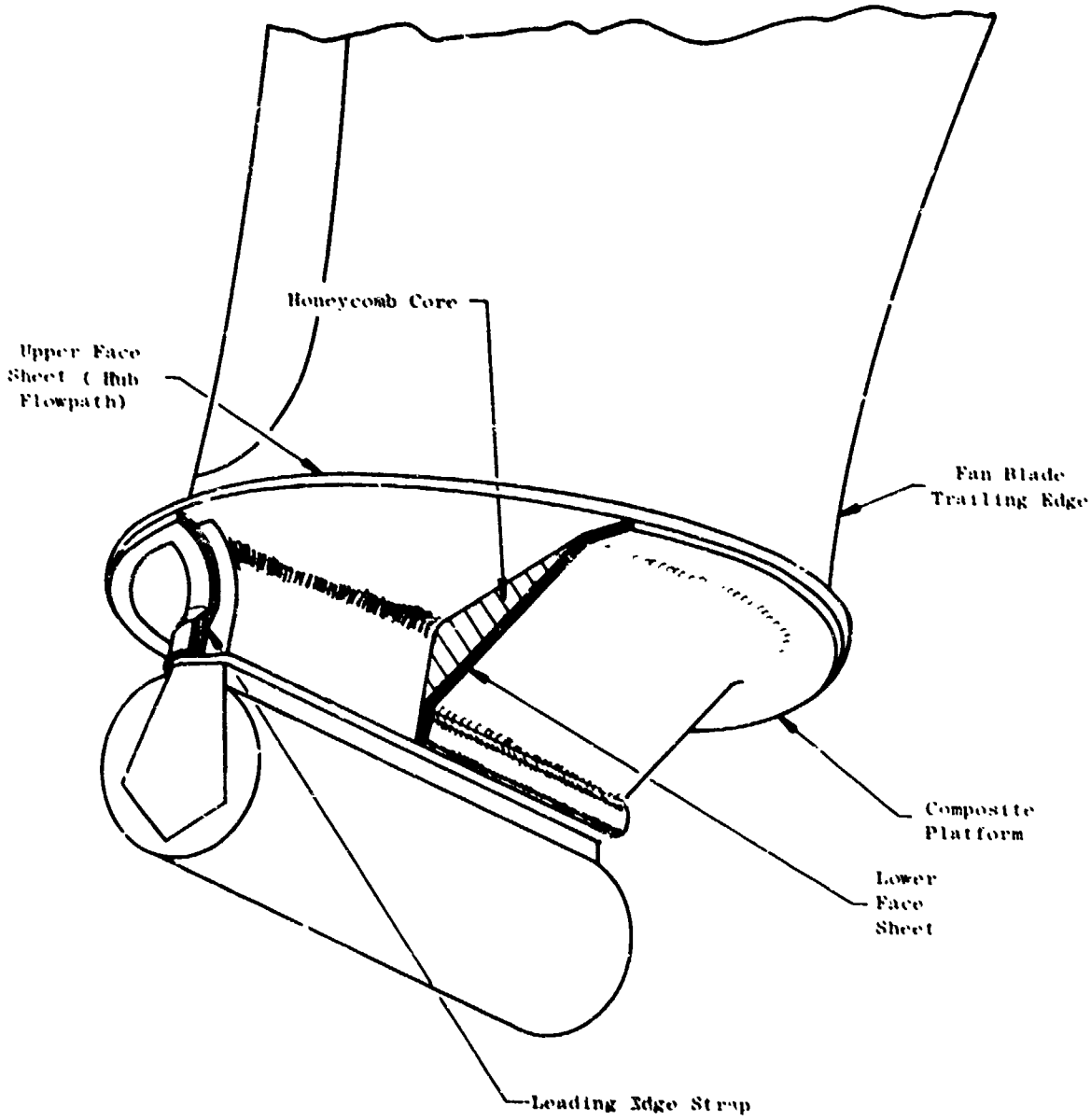

Figure 3-14. Platform Design.

SECTION 4.0

DESIGN ANALYSIS

4.1 BLADE STRESS AND DEFLECTION ANALYSIS

The blade stress analysis was performed using the 3-D finite element computer program "PARA-TAMF-EIG." This program is a parametric, 3-D, finite element eigenvalue and thermal stress computer program. The program accounts for the inertia forces of rotation and vibration. Account is taken of the stiffening effect of rotation. The program gives directly the lowest eight modes, stresses and frequencies for a specified speed of rotation. In addition, it gives deflections and stresses at any given operating rpm. The program uses an 8-noded box element (or arbitrary shape) to build up the stiffness and mass characteristics by Gaussian integration - 24 corresponding to the 3 motions at each of the eight modes and 9 internal degrees of freedom to minimize strain energy. The material properties are 3-D anisotropic. Thermal stresses are also computed. The root can be restrained by both friction and springs and distributed pressures or point forces can apply external load to the structure.

The finite element model used for the blade analysis was generated to geometrically represent the blade design. The representation required the use of 254 nodal coordinates, 105 box elements, and 7 sets of anisotropic material properties. The basic model is shown in Figure 4-1. The blade is one element thick, 8 elements wide and 11 elements tall in the airfoil region. The shank/dovetail region is one element thick, reduces to 4 elements wide and is 3 elements tall.

A number of computer runs were made to provide steady-state stresses under centrifugal and pressure loading conditions and vibratory (eigenvalue/eigenvector) relative stresses at zero and speed conditions assuming the blade dovetail to be fixed at the radial cross section corresponding to the PA plane as defined in Figure 3-10. The steady-state results at 3326 rpm (the blade duty cycle steady-state speed) show that the highest tensile stresses exist in the airfoil to dovetail transition region slightly above the leading edge undercut. The highest calculated tensile stress is 15,490 N/cm^2 (22,460 psi). The highest compressive stress is 3790 N/cm^2 (5,500 psi) at the dovetail transition trailing edge undercut. The highest calculated shear stress is 3400 N/cm^2 (4,930 psi) in the region of the leading edge overhang. Based on material development tests, the minimum expected tensile, compressive and shear strengths are 58,600 N/cm^2 (85,000 psi), 17,240 N/cm^2 (25,000 psi), 4,480 N/cm^2 (6,500 psi) providing margins of safety of 2.7, 3.5 and 0.3 respectively. The margin of safety in shear at the leading edge undercut region is expected to be improved by the addition of the platform which will share in carrying the shear loads to the dovetail. Figure 4-2 shows a plot of stresses as a function of blade span length. Figure 4-3, 4-4 and 4-5 show maximum stress and locations as well as stress maps as a percentage of maximum stress for the

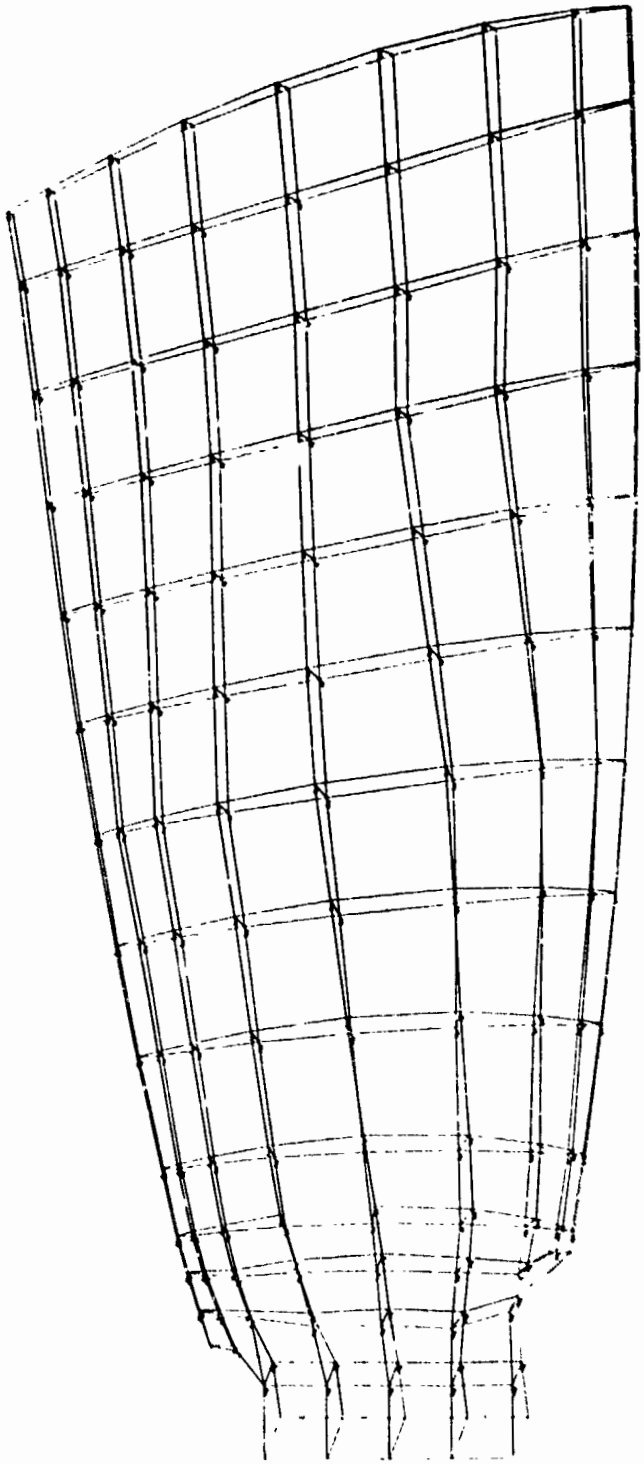

Figure 4-1. Firite-Element Model, Composite Blade.

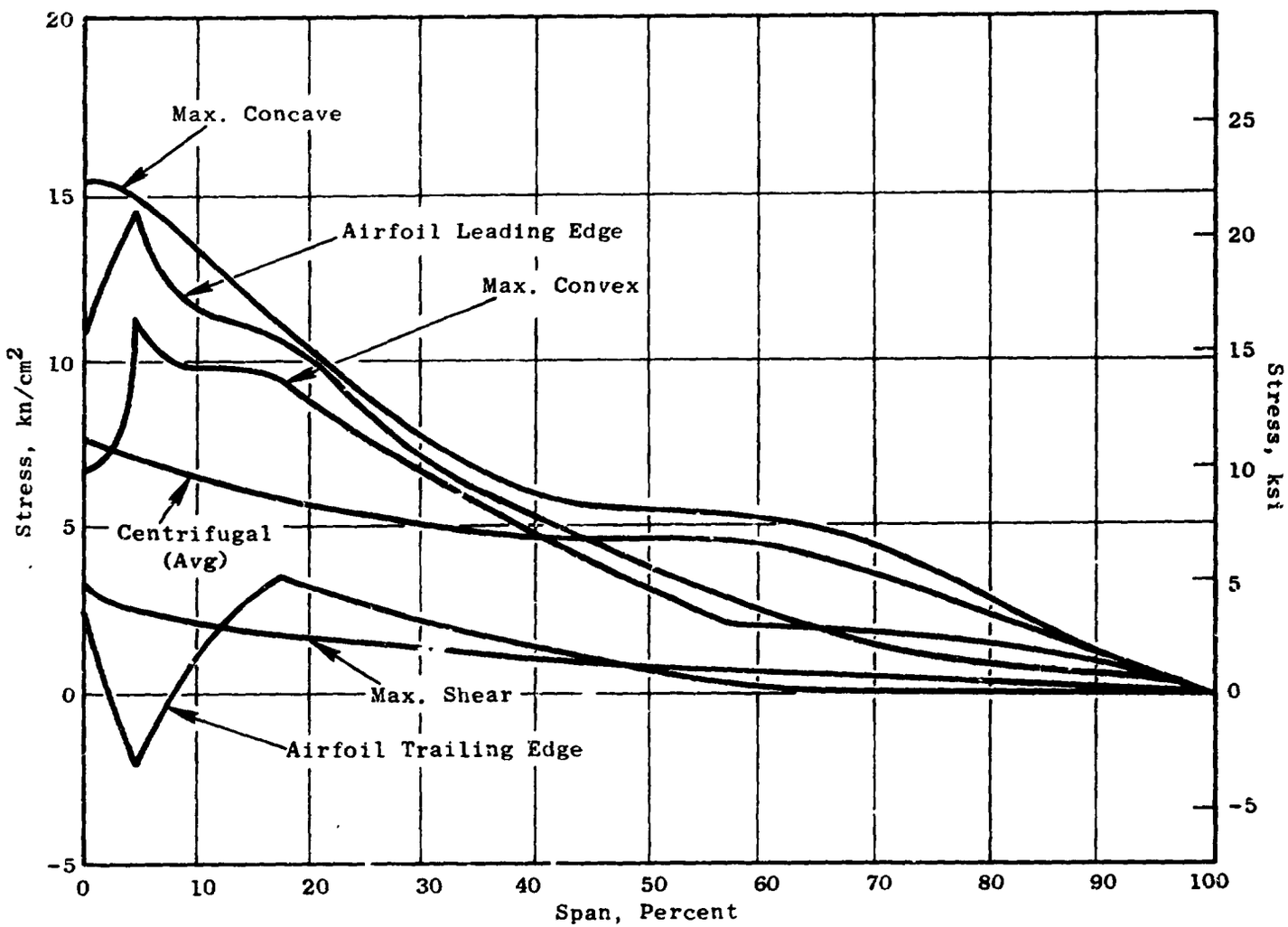

Figure 4-2. UTW Blade Resultant Radial Stress - 3326 rpm.

ORIGINAL PAGE IS
OF POOR QUALITY

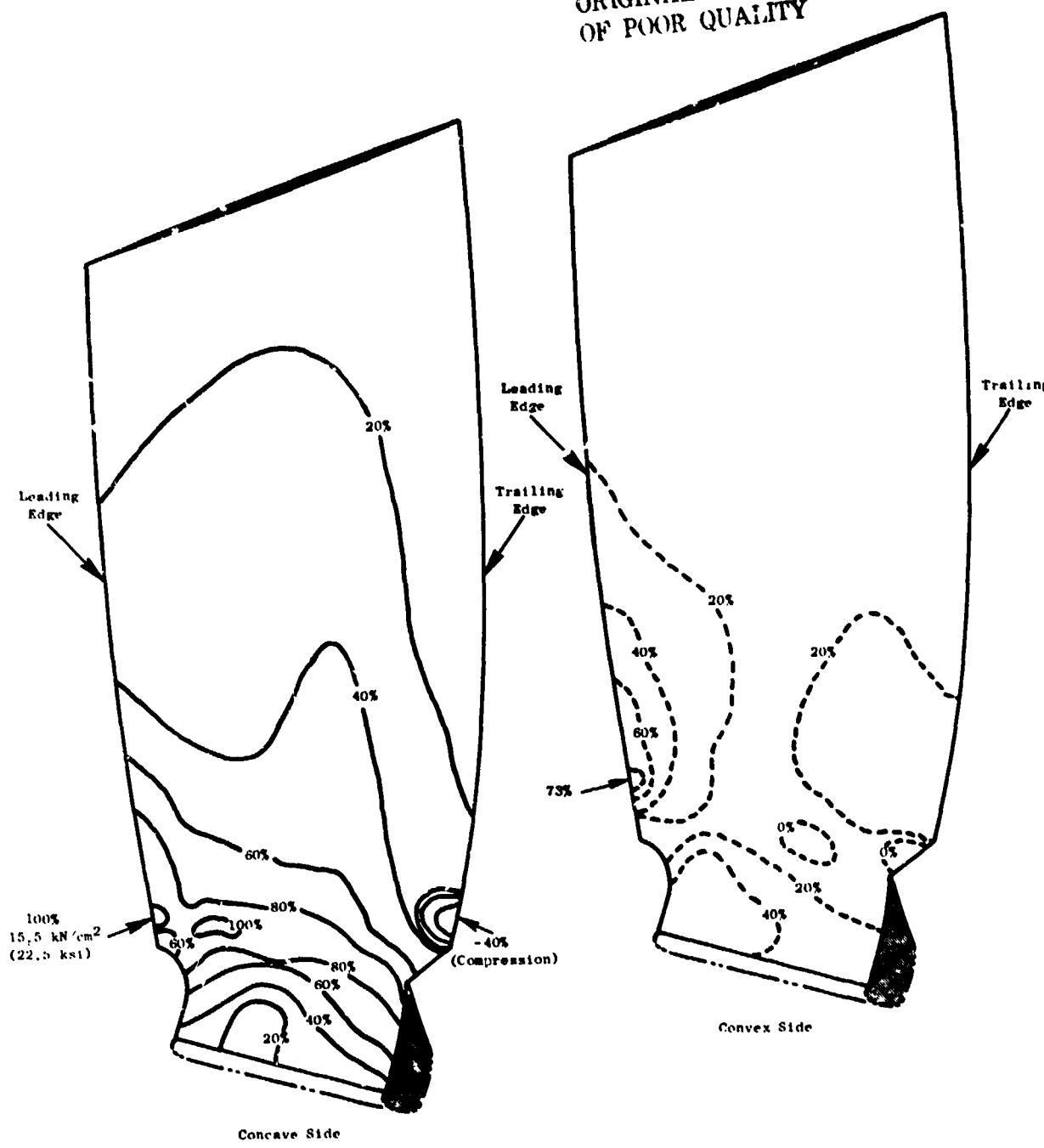

Figure 4-3. Calculated Blade Radial Stress.

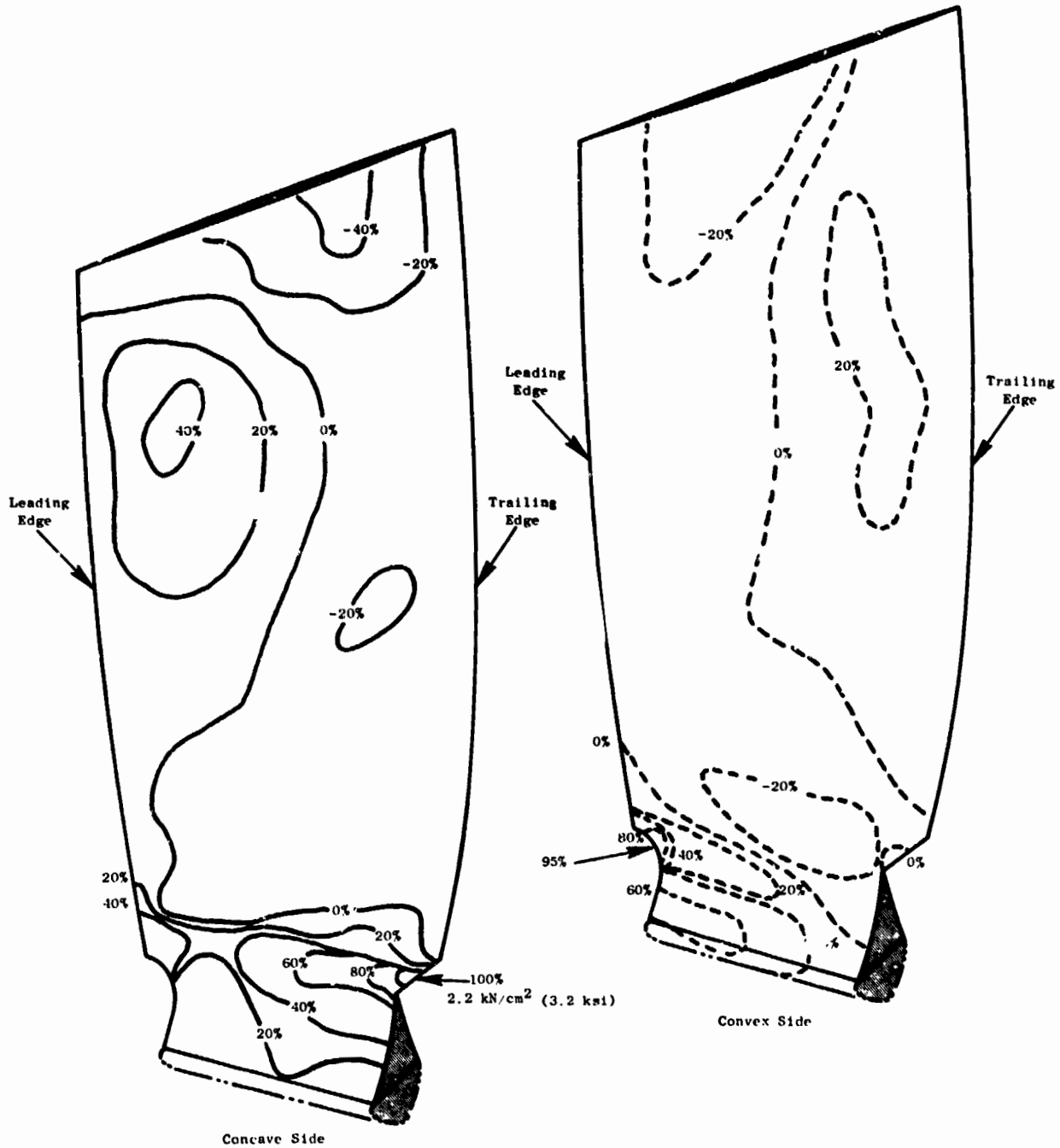

Figure 4-4. Calculated Blade Chordal Stress.

ORIGINAL PAGE IS
OF POOR QUALITY

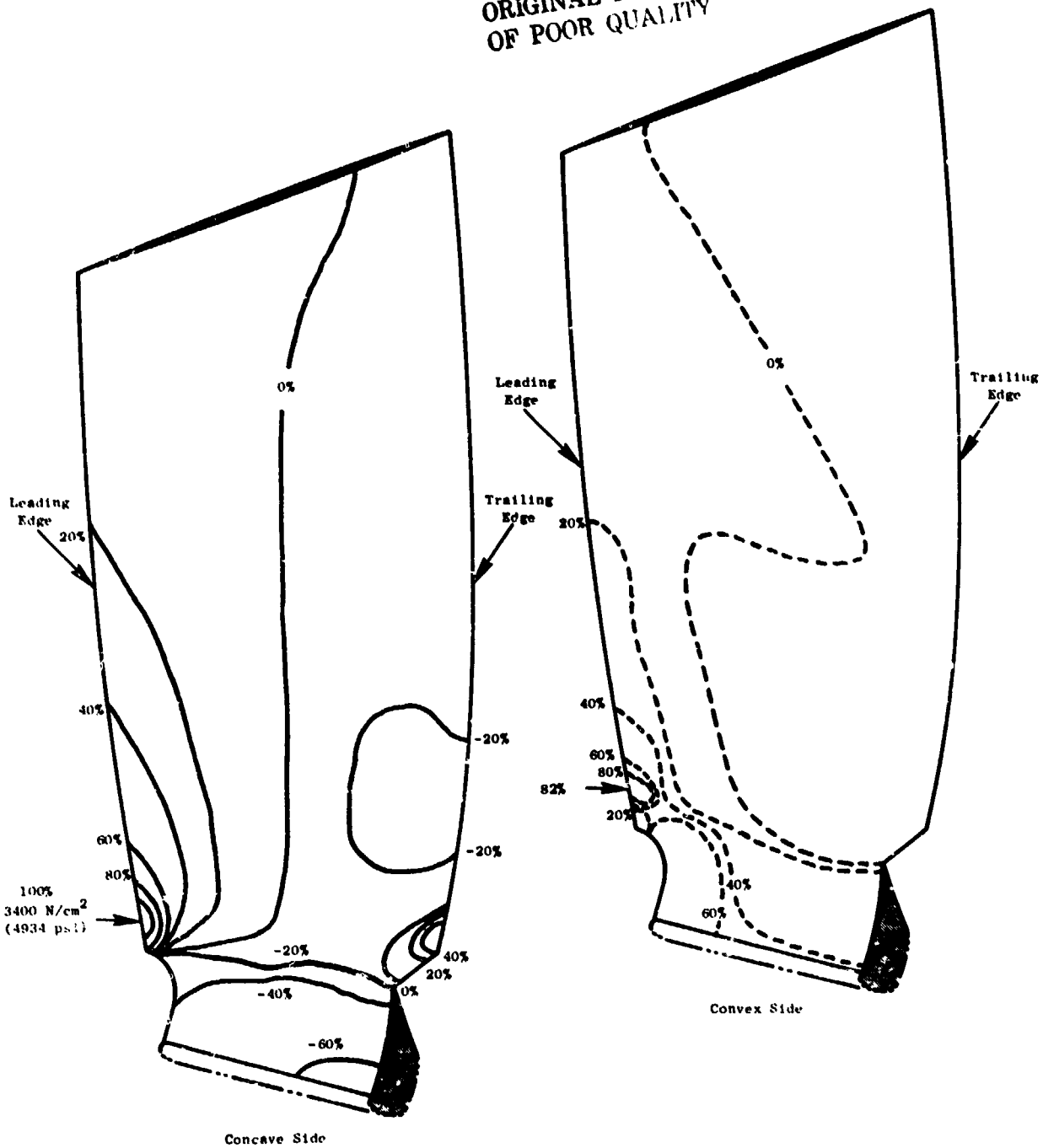

Figure 4-5. Calculated Blade Interlaminar Shear Stress.

concave and convex blade faces for radial chordwise and interlaminar shear stresses, respectively. Figure 4-6 gives a plot of blade deflection and twist as a function of span length. Figure 4-7, 4-8 and 4-9 shows relative radial stresses over the blade for the first three vibratory modes. These maps of relative radial stresses under vibratory conditions show the changes in stress locations for the different vibratory modes.

Blade vibratory strengths as determined from specimens and preliminary QCSEE blade testing are shown on the stress range diagram in Figure 4-10. The anticipated maximum vibratory stress is 11 ksi single amplitude on the basis of testing on other engine programs. For the steady-state conditons shown, that of a hot day takeoff and maximum standard day cruise, the combination of steady-state mean stress and expected maximum vibratory stress results in an acceptable blade life.

The blade composite dovetail stresses were determined using the radial load distribution from the above blade analysis and experimental data from previous 2-D dovetail specimens and blade testing. Maximum dovetail crushing stress is calculated to be 15,290 N/cm^2 (22,180 psi) and maximum dovetail calculated shear stress is 4,760 N/cm^2 (6,900 psi) at a blade speed of 3326 rpm. Based on dovetail development tests, the expected minimum dovetail crushing and shear strengths are 55,160 N/cm^2 (80,000 psi) and 16,550 N/cm^2 (24,000 psi) respectively showing adequate static strength margins of safety in each case. These strengths were further verified by two blade-dovetail pull tests which demonstrated corresponding minimum crushing and shear strengths of 56,750 N/cm^2 (82,300 psi) and 17,650 N/cm^2 (25,600 psi) respectively. It is expected that these strengths would actually be higher in that the test load reached the capability of the loading fixture without dovetail failure.

The dovetail vibratory strengths were projected from previous composite experimental data and the QCSEE dovetail static strength data. Figure 4-11 shows the allowable stress range diagram for dovetail crushing and Figure 4-12 shows the allowable stress range diagram for dovetail shear. The anticipated maximum single amplitude vibratory stresses are 5,580 N/cm^2 (8,100 psi) in crushing and 2,340 N/cm^2 (3,400 psi) in shear and are based on the anticipated maximum blade radial vibratory stresses. For the steady-state conditons shown, that of hot day takeoff and maximum cruise, the combination of steady-state mean stress and expected maximum vibratory stress results in an acceptable dovetail life.

4.2 PLATFORM STRESS AND VIBRATION ANALYSIS

The analytical approach used in evaluating the platform was to calculate the stresses and mechanical frequencies using simple conservative models of unit width cross sections representing the platform design. The stress were calculated for the platform operating in the 5259 "G" centrifugal force field resulting from 100% speed operation at 3326 rpm. Positive margin at a 41% overspeed conditon of 4700 rpm is met by maintaining a margin of safety, MS = 2 at 3326 rpm. As a further precaution to guard against a possible

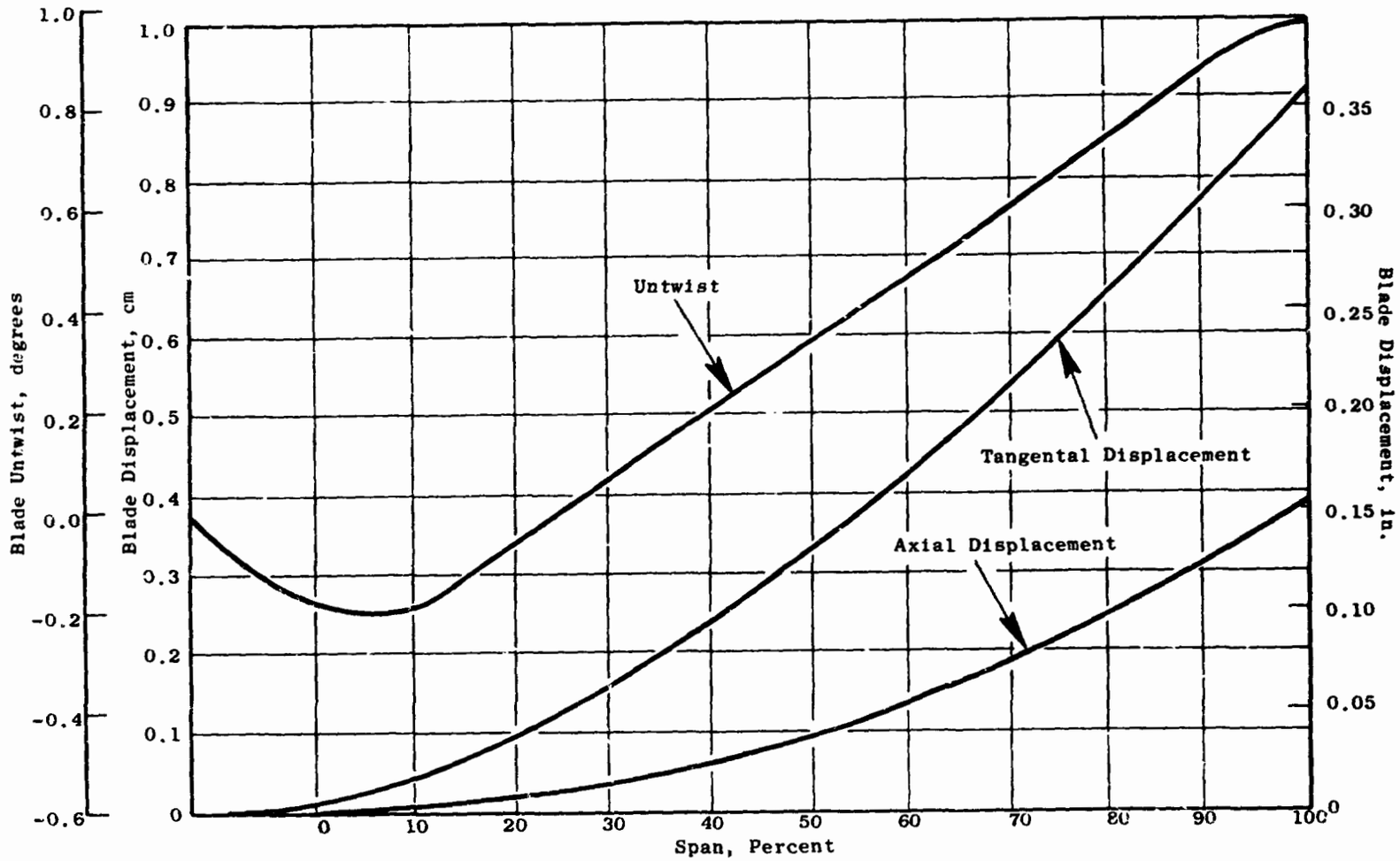

Figure 4-6. UTW Blade Displacements and Twist.

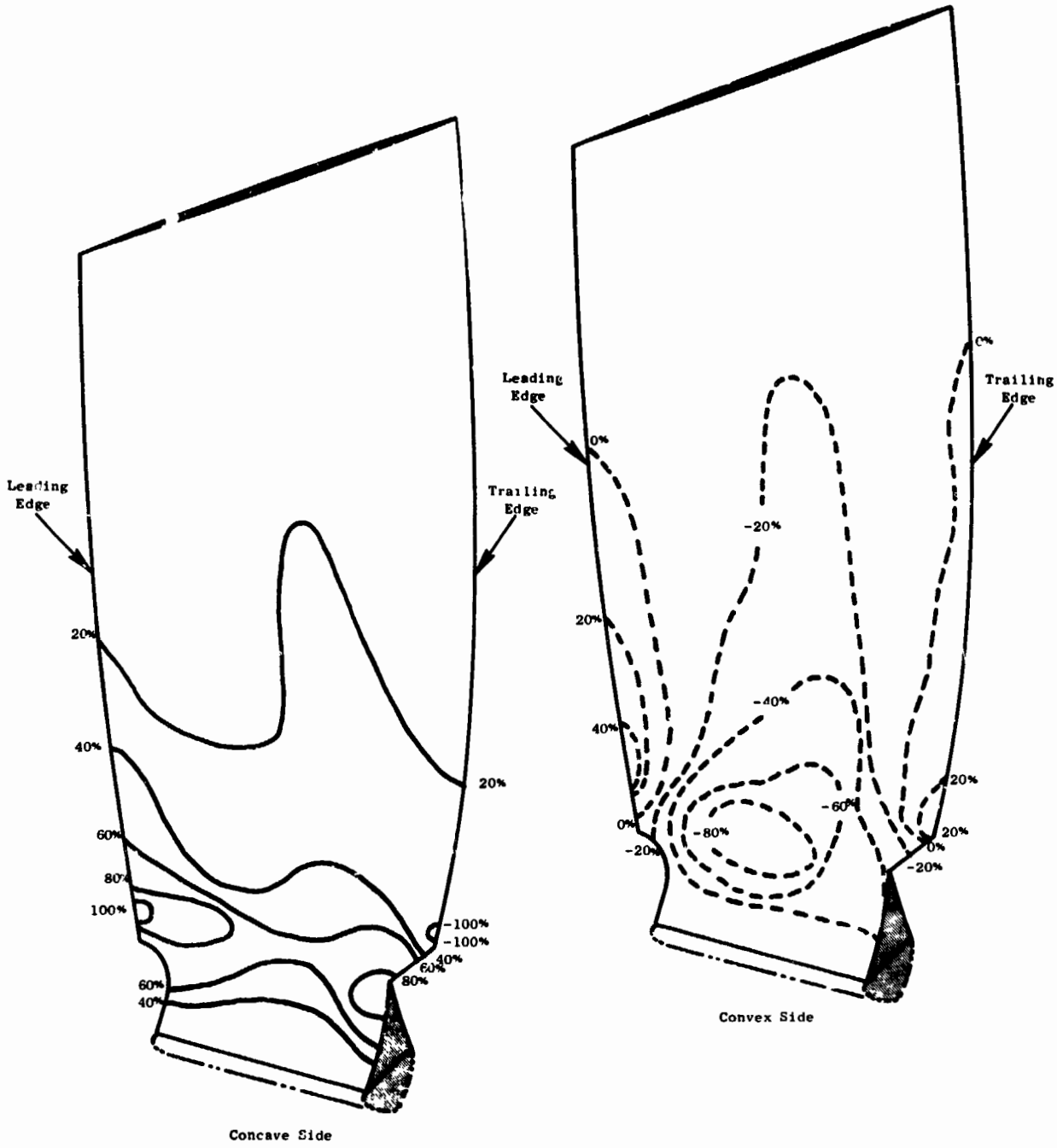

Figure 4-7. Calculated Blade Relative Radial Stresses for First Flexural Mode.

ORIGINAL PAGE IS
OF POOR QUALITY

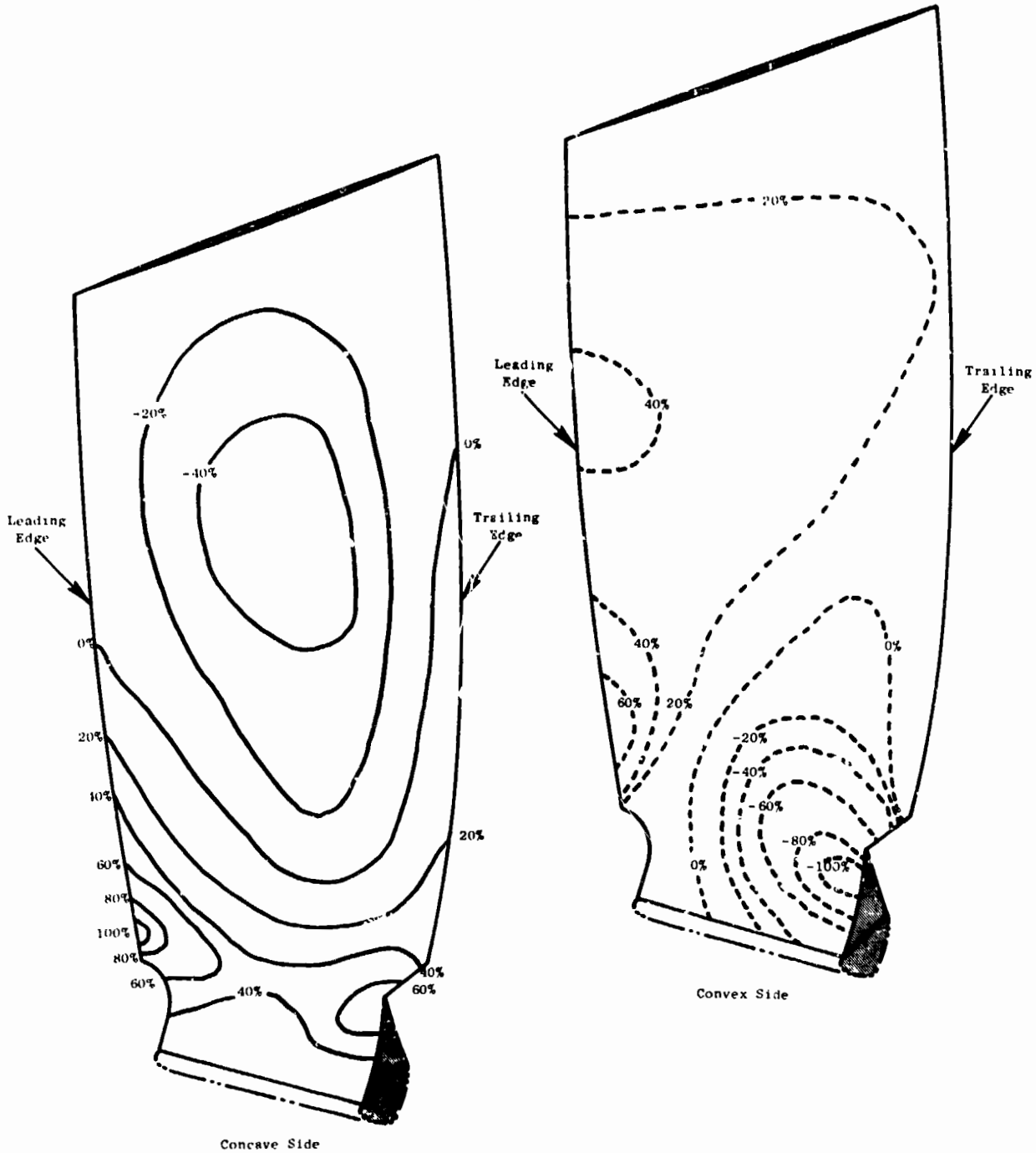

Figure 4-8. Calculated Blade Relative Radial Stresses for Second Flexural Mode.

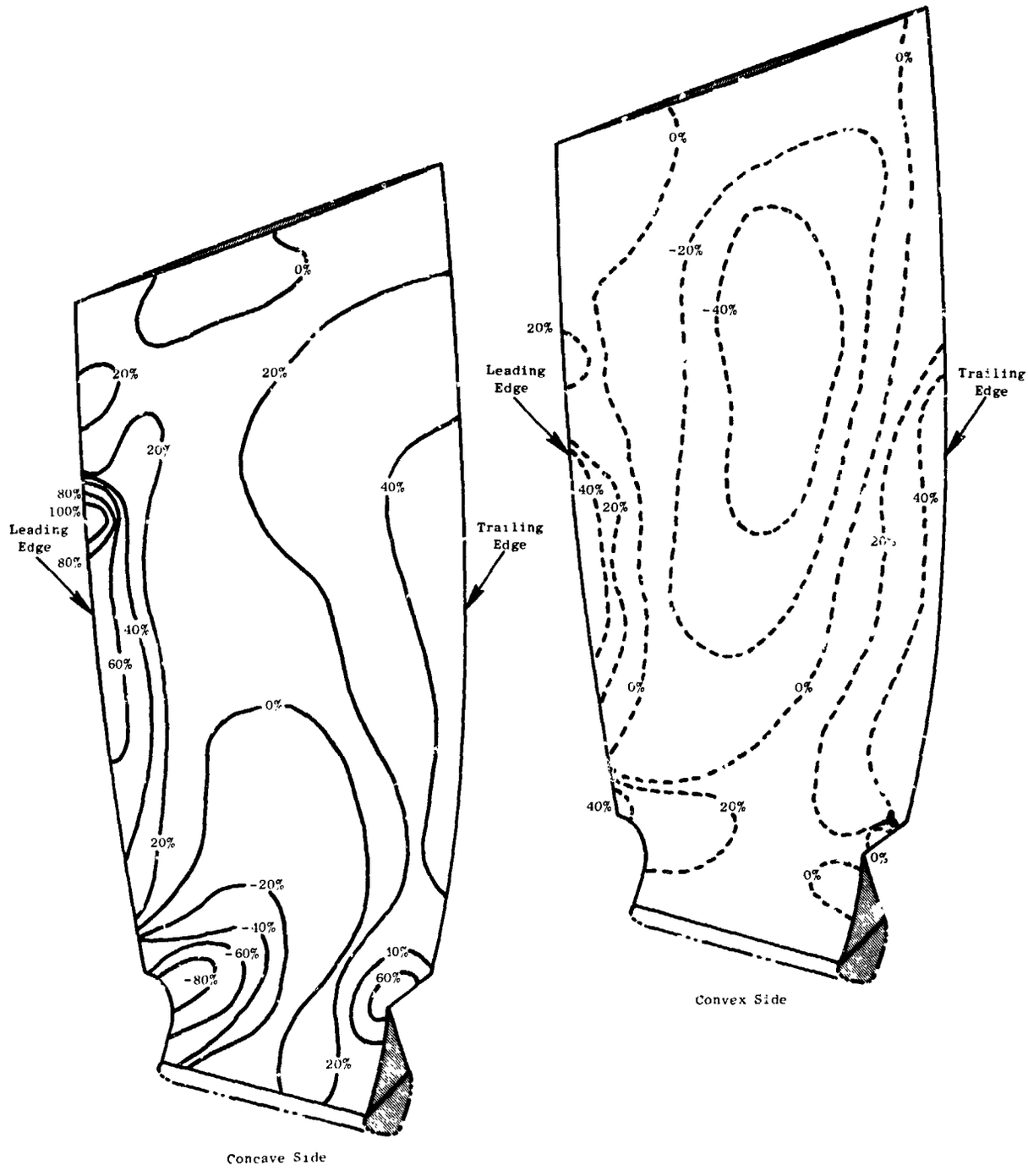

Figure 4-9. Calculated Blade Relative Radial Stresses for First Torsional Mode.

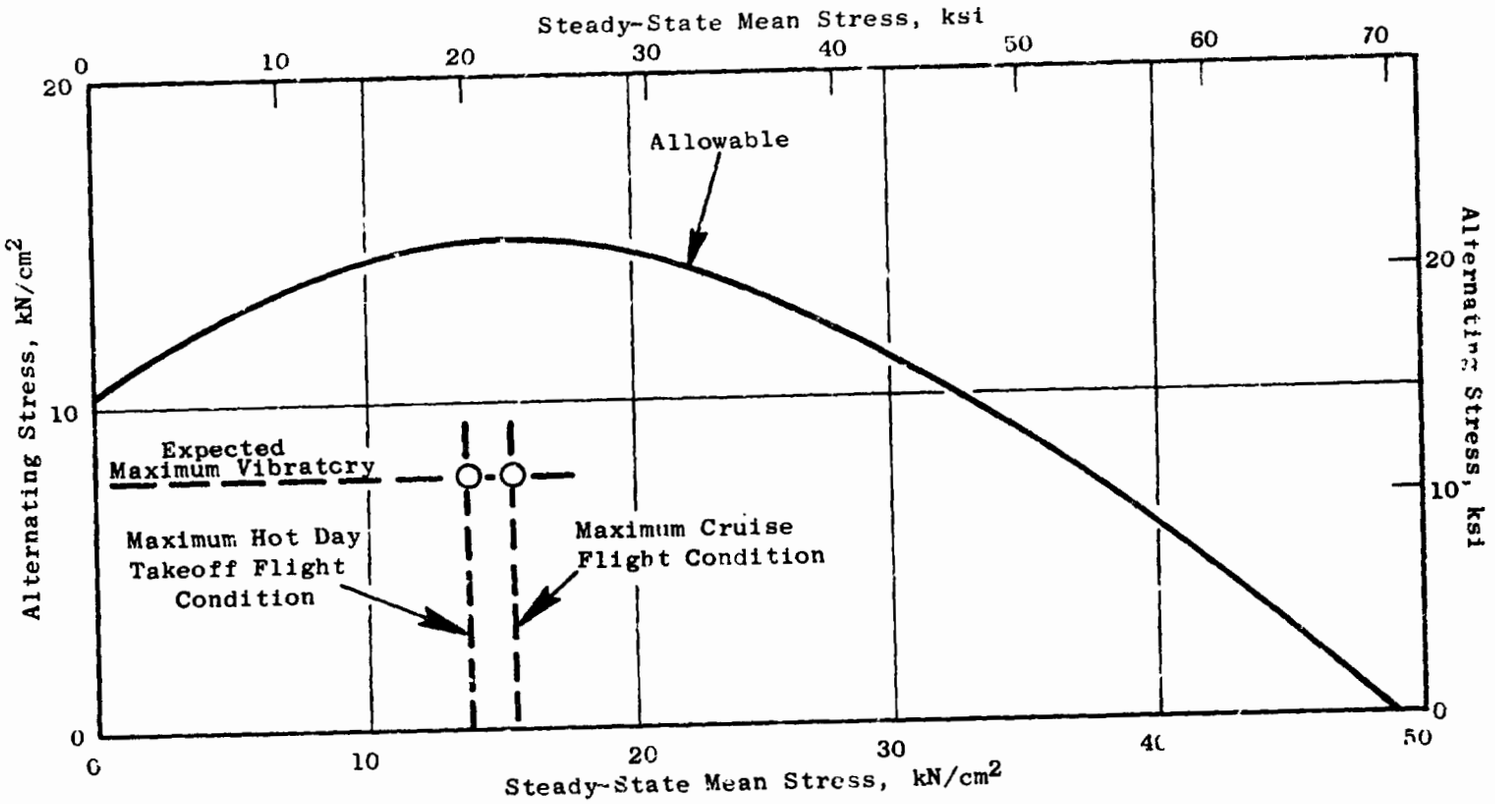

Figure 4-10. Allowable Stress Range Diagram - Blade Radial Stress

ORIGINAL PAGE IS
OF POOR QUALITY

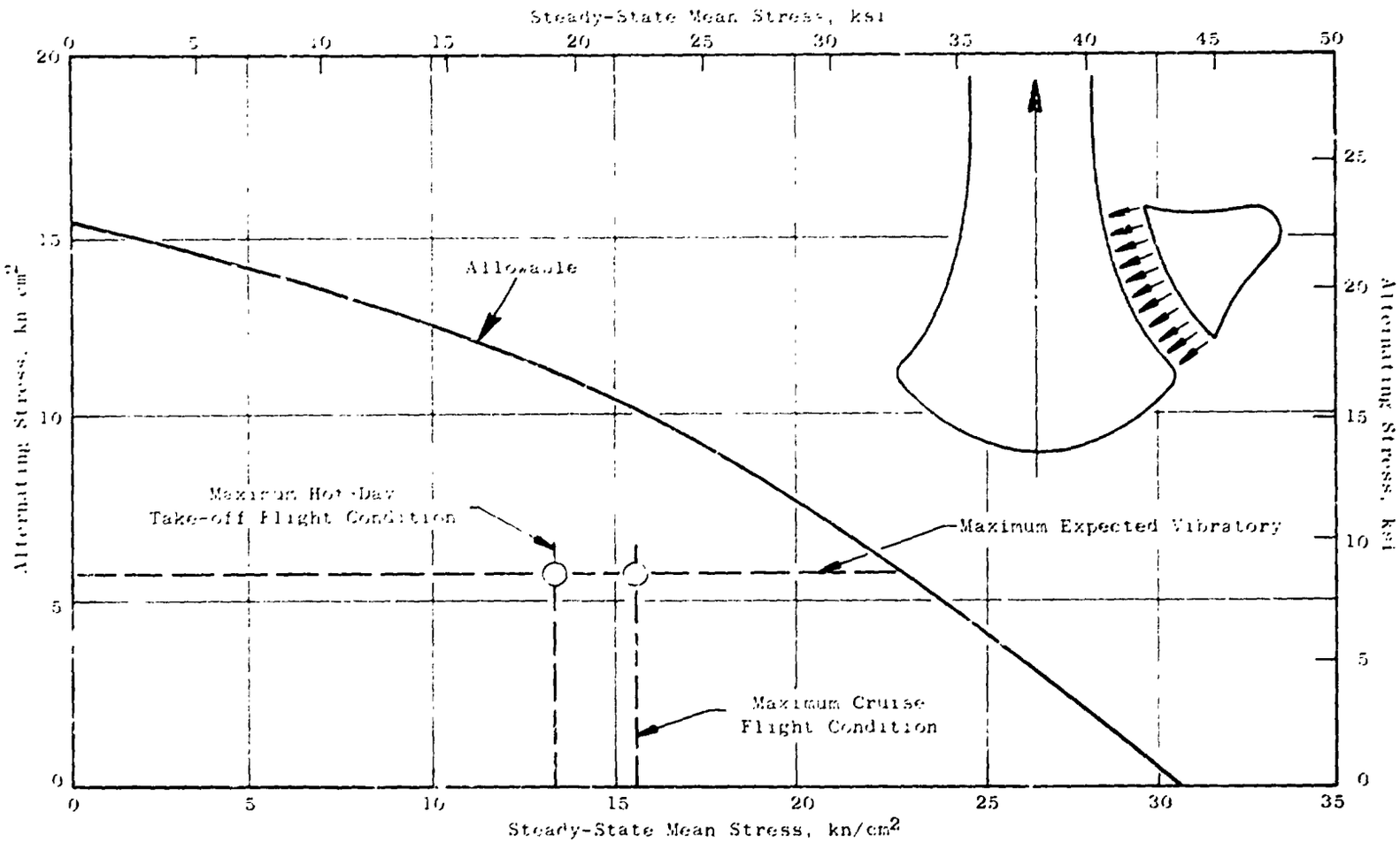

Figure 4-11. Allowable Stress Range Diagram - Blade Radial Stress.

ORIGINAL PAGE IS
OF POOR QUALITY

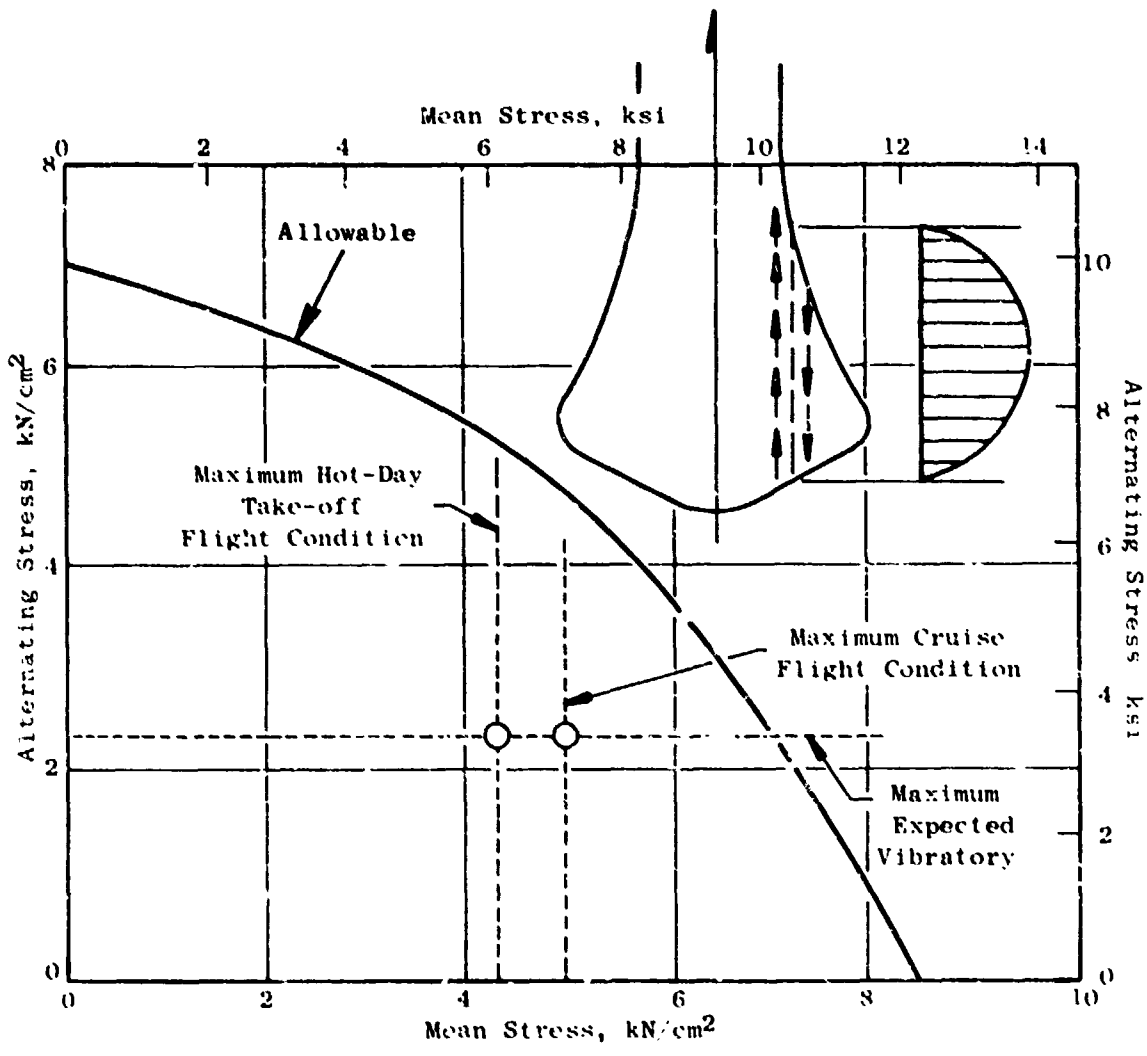

Figure 4-12. Allowable Stress Range Diagram - Dovetail Shear Stress.

material property loss from the planned manufacturing co-curing process, only 70% of the published material allowable is used.

Figure 4-13 shows a cross section of the platform. Since the outerface sheet (location 5 flowpath surface, Figure 4-13) is an eccentric compressively loaded sheet operating in a centrifugal force field producing lateral loading, and is stabilized by the honeycomb bond, it has been investigated for its beam-column capability. It is designed to be adequate even with a partial loss of honeycomb bond. For correlation with the analysis and to investigate various alternate design features, typical platform sections have been manufactured and tested. The testing has supported the analytical findings and at location 3 has identified the load carrying capability to be greater than 490 N/cm (280 lb/in.) normal to the blade centerline. This has allowed a MS = 2 at location 3 to be identified by test where an otherwise difficult analysis would be required to identify the maximum stress. A stress and margin of safety summary is presented in Table 4-I for 6 points of interest.

The platform vibratory characteristics are investigated from three points of view. First, the platform is considered cantilevered from the blade. Second, as a member running from fore to aft, it is considered free from the blade to flex in a free-free (floating) condition, and in the tangential direction (still free from the blade) it is considered to be cantilevered from the leading and trailing edge straps. Third, the upper face sheet with a partial loss of the honeycomb bond is considered. The first natural frequency for these various models are tabulated in Table 4-II.

The platform is stiffer than any of the models used to calculate the first natural frequency. Therefore, the platform's first natural frequency is higher than those calculated and will be above the excitation frequencies of the blade.

The platform weight at less than .16 kg (.35 lb.) is composed of 20% honeycomb, 10% adhesive and 70% graphite/epoxy composite. It is fabricated in one piece which is simultaneously molded and bonded onto the composite blade using a co-curing process. The upper face sheet or flowpath contour is controlled by a hard die fitted around the blade. The graphite/epoxy upper face sheet is layed-up on the contour formed by the die and blade root surface. A contoured aluminum honeycomb core is next put in place followed by the lower face sheet layed-up on the honeycomb core. The layed-up assembly is then put into a vacuum bag and the entire assembly is co-cured onto the blade. The result is a one piece platform design. The outer contour of the platform overhang is then trimmed to final dimensions.

4.3 BLADE VIBRATION ANALYSIS

Blade "instability" or "limit cycle vibration" can be a problem on fans. It is characterized by a high amplitude vibration in a single mode (normally the first flexural or torsional mode) at a nonintegral per-rev frequency. Because of the nonlinearity in the aerodynamics involved, it has resisted satisfactory solutions by solely theoretical means. Accordingly, General Electric

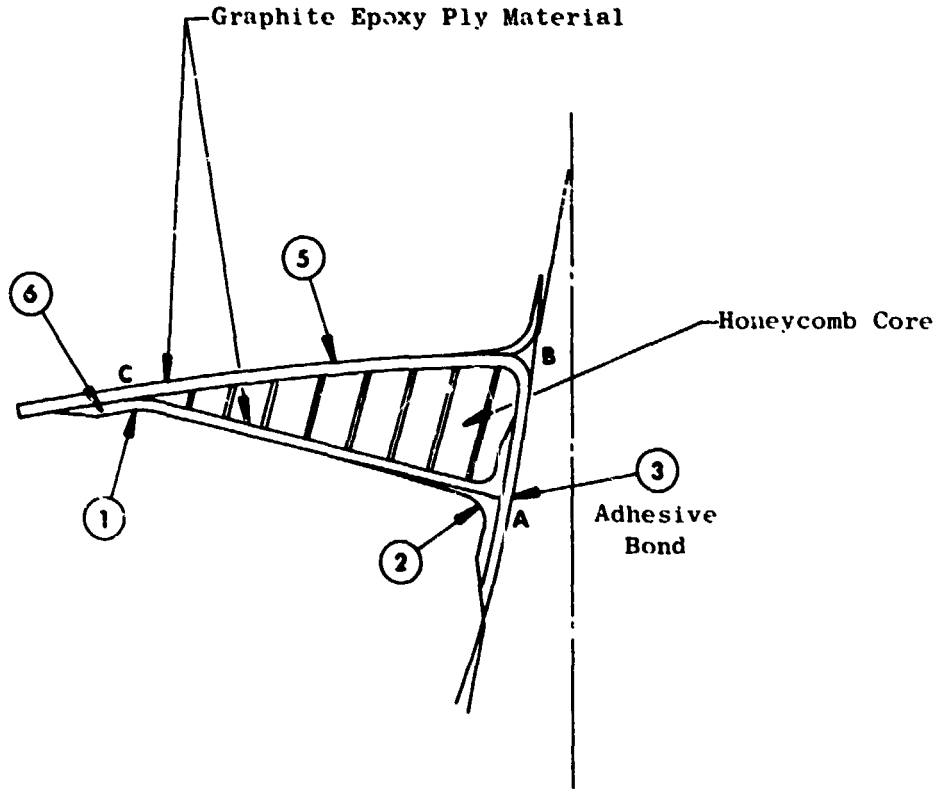

Figure 4-13. Platform Cross Section.

Table 4-I. Platform Stresses and Margins of Safety.

Location of Interest	Description and Type of Stress	Stress kN/cm^2 (ksi)	Margin of Safety
1	Flexural Stress in Overhand up to 2.5 cm (1 Inch) with Additional Single Thickness Overhang up to 1 cm (.400 Inch)	$\sigma \leq$ 16.5 (24)	> 2.0
2	Tensile Stress in Lower Face Sheet	$\sigma <$ 13.8 (20)	> 2.2
3	Tensile Stress Capability at This Location is Correlated with Test Results	-	> 2.0
4 Not Shown	Tensile Stress in Leading Edge Strap	$\sigma \leq$ 13.8 (20)	> 2.0
5	Combined Compression and Flexural Stress in Upper Face Sheet	$\sigma \leq$ 24 (35)	> 2.0
6	Shear Stress Between Upper and Lower Face Sheets	$\tau <$ .05 (.07)	> 2.1

Table 4-II. Platform Natural Frequencies.

Models Considered	First Natural Frequency
Cantilever (Platform)	$f_1 > 5000$ Hz
Cantilever (Platform Overhang)	$f_1 > 2000$ Hz
Free-Free (Platform)	$f_1 > 8000$ Hz
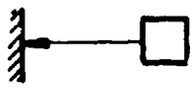 Cantilevered Mass (End Straps Supporting a Free Platform)	$f_1 > 1500$ Hz
Clamped Beam (Face Sheet Partial Loss of H/C Bond)	$f_1 > 1500$ Hz

has adopted a semiempirical "reduced velocity parameter" approach for limit cycle avoidance. Reduced velocity parameter, V_R, gives a measure of a blade's stability against self excited vibration. This parameter is defined as

$$V_R = \frac{W}{bf_t}$$

where:

b = 1/2 chord at 5/6 span-m

W = average air velocity relative to the blade over outer third of the span-m/sec

f_t = first torsional frequency at design rpm-rad/sec.

The basic criterion used to select the design of the UTW composite blade was the requirement of having a reduced velocity parameter in the range of 1.3 to 1.4. This allowable range is based on previous testing of a variety of fan configurations in combination with the specific aerodynamic design of the UTW blade. The 18-blade design using a hybrid of boron, graphite, Kevlar-49 and glass material was selected as providing the desired aeromechanical requirements. The operating and stall characteristics of this blade are presented in Figure 4-14 in terms of reduced velocity versus incidence angle. This shows the capability of reaching full rotating stall prior to encountering blade instability.

The Campbell diagram for the UTW blade assembled in the trunnion and disk is shown in Figure 4-15. The coupled frequency of the blade-trunnion assembly, as plotted here, is somewhat lower than the individual blade frequencies due to the flexibility of the supporting trunnion and disk. The expected first flexural frequencies at 2/rev crossover is shown to be at 67% speed. This is above the engine flight idle speed and below the normal operating speed for takeoff, climb and max cruise flight conditions, therefore, is a transient point in the flight mission and not subject to continuous steady-state conditions. Blade excitation stresses at 2/rev crossover will be monitored during engine testing. Blade pitch changes and speed changes will be employed if they should become excessive.

The margin for first flexural frequency over 1/rev at 115% speed is approximately 50%, and the margin for first flexural frequency below 2/rev at 100% speed is approximately 13%.

The second flexural mode crosses several per/rev lines in the operating speed range. Each of these crossings represent a potential for forced resonances, however, it takes considerably more energy to drive the higher vibration frequencies such as second flex and no problems are anticipated.

The first torsional frequency 6/rev crossover is at approximately 83% speed with the 100% speed frequency margin being approximately 6% over 5/rev.

ORIGINAL PAGE IS
OF POOR QUALITY

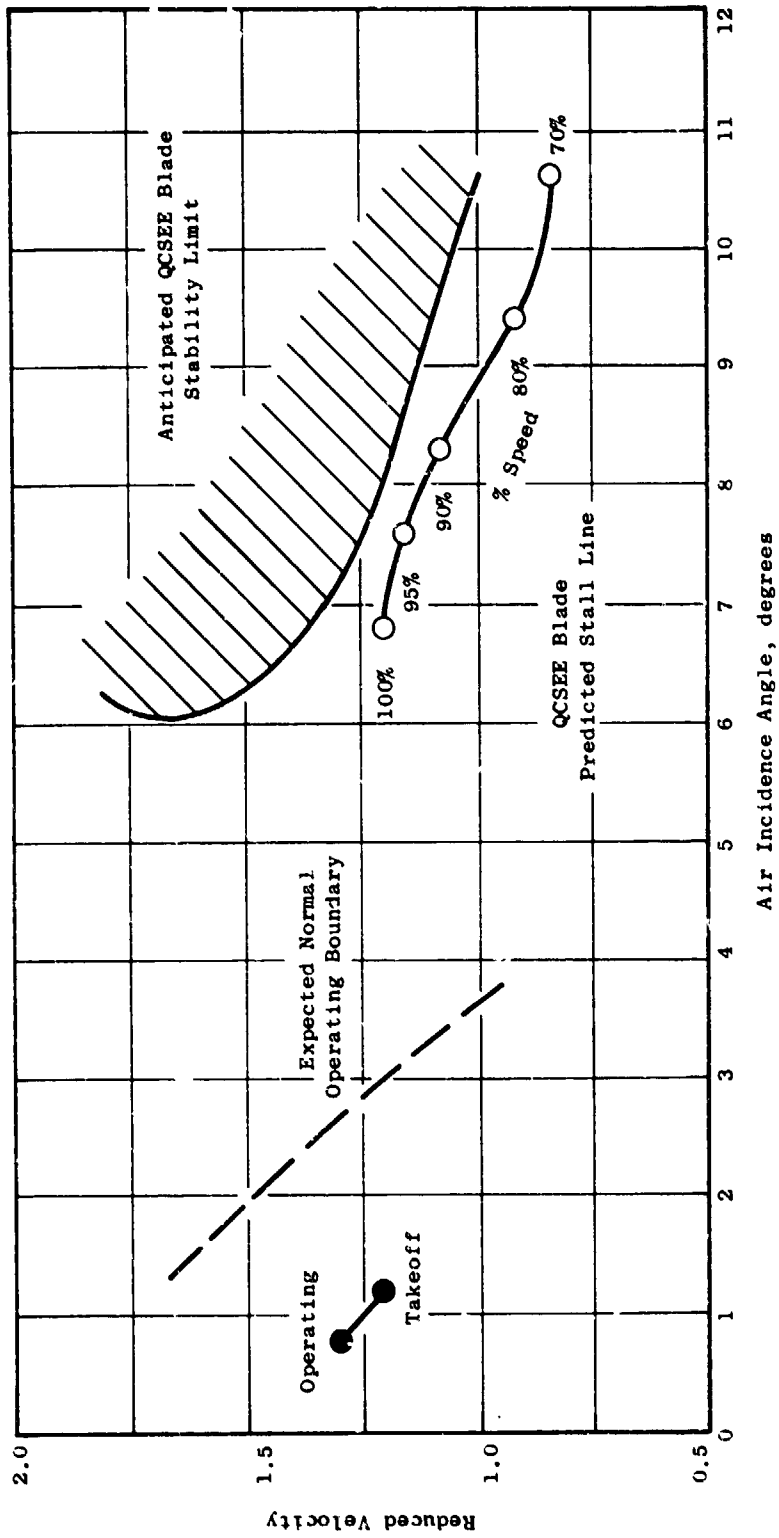

Figure 4-14. Limit Cycle Boundaries.

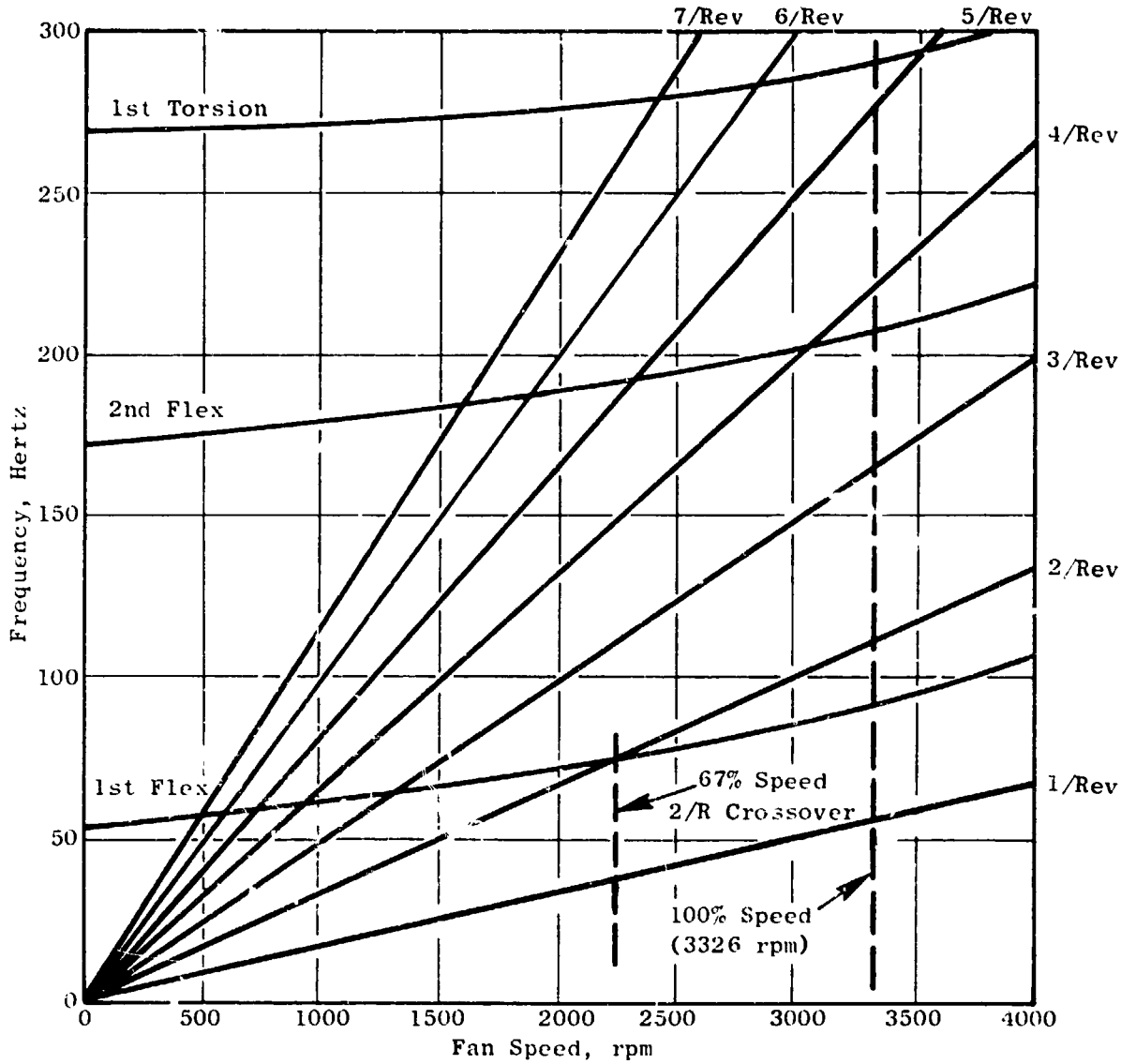

Figure 4-15. Campbell Diagram - UTW Composite Blade.

Since the excitation forces should be small at the higher order crossovers, no vibratory problems are anticipated during normal engine operating conditions.

4.4 BLADE IMPACT ANALYSIS

In addition to the aeromechanical consideration of satisfying flutter requirements, designing for bird impact resistance is also of major importance. Flight engine QCSEE blades will be required to absorb the impact of sixteen .09 kg (3 oz) birds, eight .68 kg (1-1/2 lb.) birds, and a 1.8 kg (4 lb.) bird in order to satisy FAA specifications. The objectives are to sustain little or no damage during starling ingestion, be able to maintain 75% engine thrust following .68 kg (1-1/2 lb.) bird ingestion and to be able to have a safe engine shutdown with all damage being contained within the engine casing following a 1.8 kg (4 lb.) bird ingestion.

Two different damage modes require consideration in the design. The first is a brittle root type fracture which can result in the blade breaking off close to the dovetail and the second is local damage which can result in airfoil delamination and a loss of materials.

The projected elimination of root failures during large bird impact in the QCSEE blade has been achieved by a combination of judicious airfoil and dovetail design. More flexibility and strain-to-failure capability has been built into the blade root through the use of hybrid materials. The dovetail design provides for energy dissipation through centrifugal recovery and increase in friction energy. Figure 4-16 illustrates the magnitude of energy that has to be absorbed by the blade at the root, tip, and pitch for the spectrum of relative bird velocities for a 1.8 kg (4 lb.) bird. This shows that the most vulnerable condition and blade impact loaction is during climb at approximately 91.4 m/sec (300 ft/sec) and at the blade 50% span location, respectively. The gross i[illegible] capability of the QCSEE blade is shown in Figure 4-17. This shows the advantages of the QCSEE dovetail attachment and the use of hybrid materials over the previous fixed-root solid graphite-type blade. The magnitude of the impact loading can be calculated in terms of momentum. Figure 4-18 shows a plot of projectile normal momentum for a .68 kg (1-1/2 lb.) bird at the blade 50% and 75% span locations as a function of airplane speed.

4.5 WEIGHT

The weight of the composite blade was computed using the final blade configuration as shown in Figure 3-7. This weight breakdown is shown in Table 4-III.

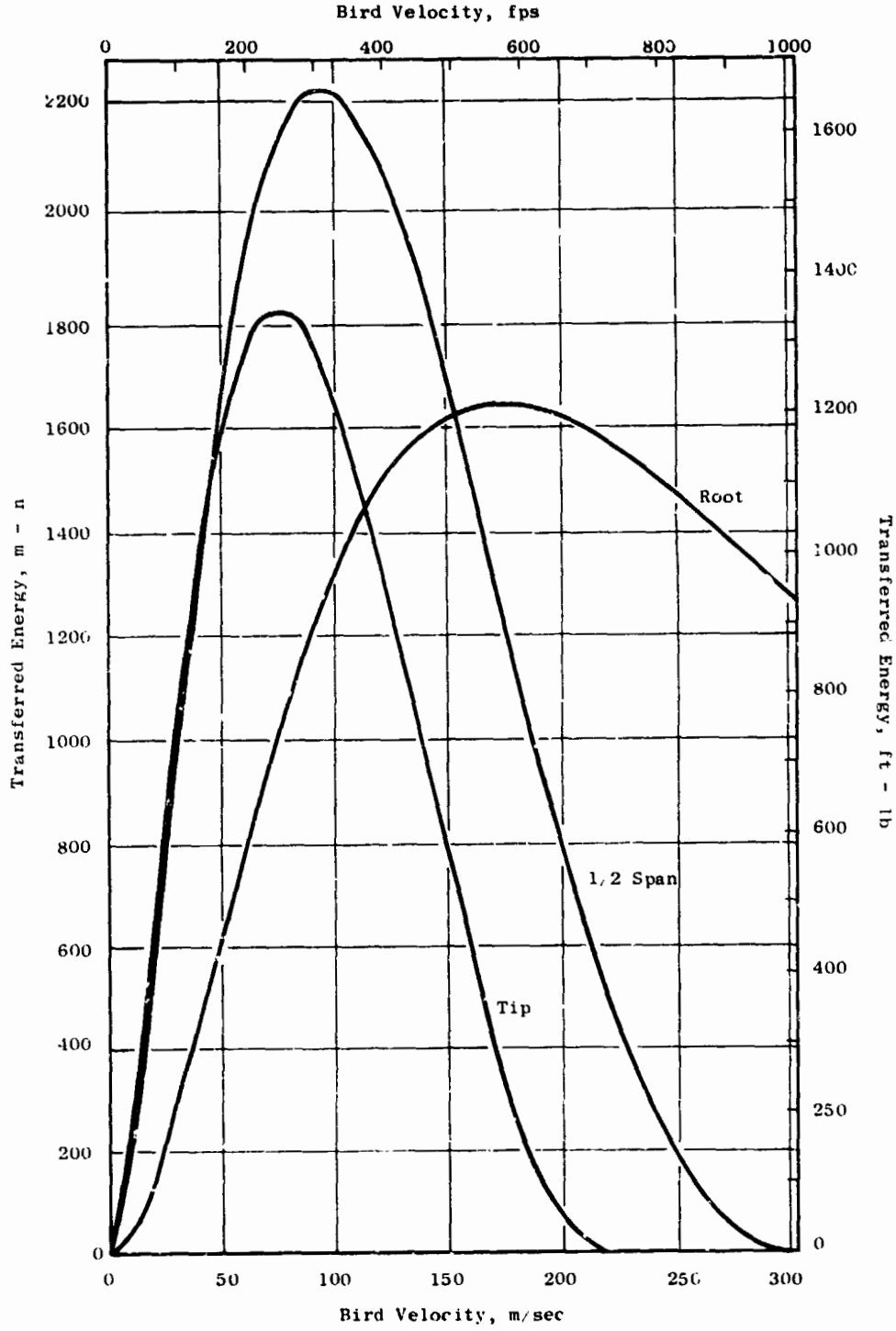

Figure 4-16. UTW Blade Transferred Impact Energy for a 1.81 kg (4 lb) Bird.

ORIGINAL PAGE IS
OF POOR QUALITY

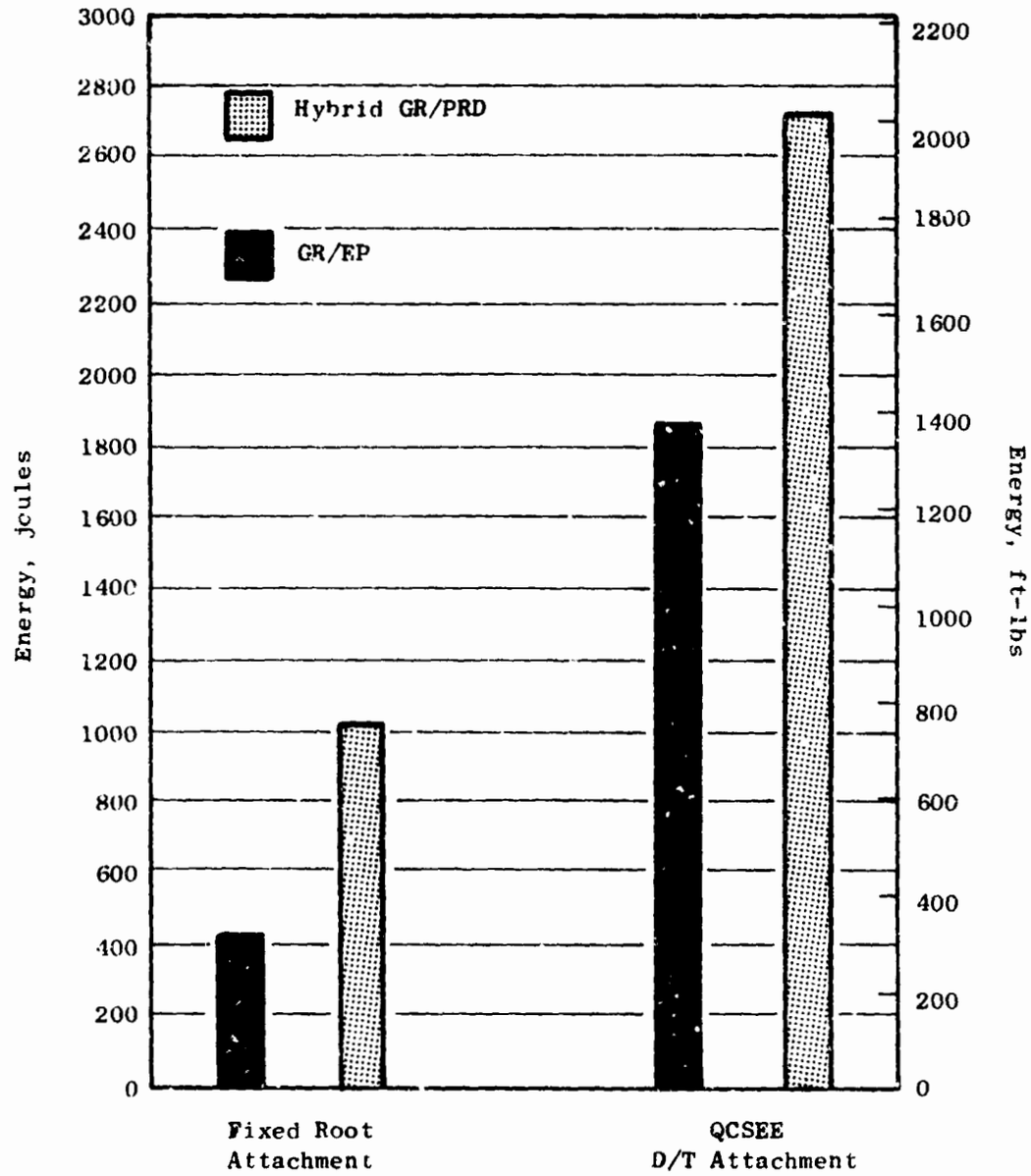

Figure 4-17. QCSEE Composite Blade Predicted Gross Impact Capability.

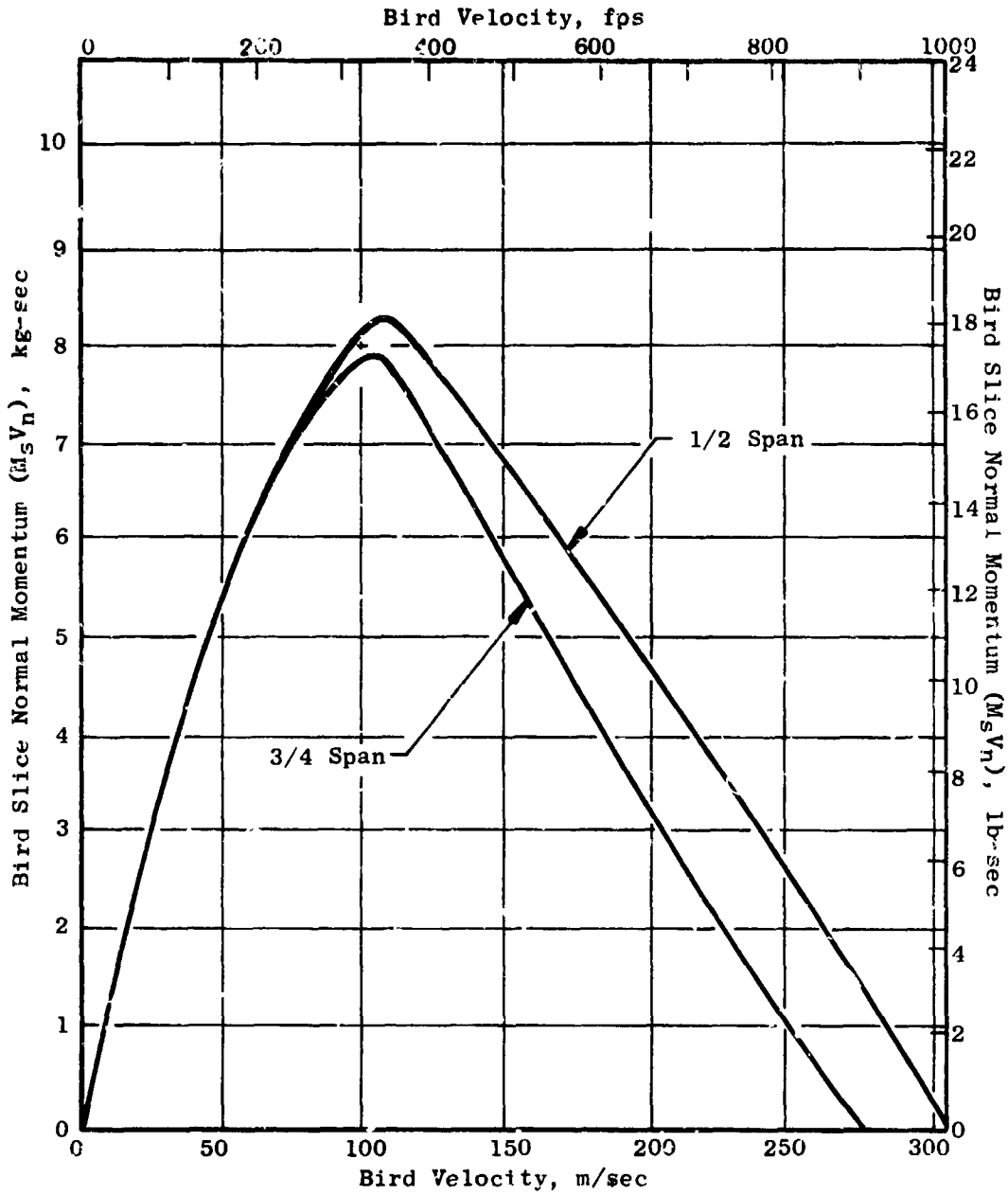

Figure 4-18. UTW Blade Impact Momentum for a 0.68 kg ($1\frac{1}{2}$-lb) Bird.

Table 4-III. UTW Composite Blade Weight Summary.

	Weight	
	kg.	lb.
Composite	1.74	3.83
Leading Edge Protection	.20	.45
Polyurethane Coating	.07	.15
Platform and Adhesive Bond	.15	.34
Dovetail	.47	1.03
TOTAL WEIGHT	2.63	5.80